

Review

Microbial Fuel Cell for Energy Production, Nutrient Removal and Recovery from Wastewater: A Review

N. Evelin Paucar * and Chikashi Sato

Department of Civil and Environmental Engineering, Idaho State University, 921 S. 8th Ave., Stop 8060, Pocatello, ID 83209, USA; satochik@isu.edu

* Correspondence: paucnori@isu.edu

Abstract: The world is facing serious threats from the depletion of non-renewable energy resources, freshwater shortages and food scarcity. As the world population grows, the demand for fresh water, energy, and food will increase, and the need for treating and recycling wastewater will rise. In the past decade, wastewater has been recognized as a resource as it primarily consists of water, energy-latent organics and nutrients. Microbial fuel cells (MFC) have attracted considerable attention due to their versatility in their applications in wastewater treatment, power generation, toxic pollutant removal, environmental monitoring sensors, and more. This article provides a review of MFC technologies applied to the removal and/or recovery of nutrients (such as P and N), organics (COD), and bioenergy (as electricity) from various wastewaters. This review aims to provide the current perspective on MFCs, focusing on the recent advancements in the areas of nutrient removal and/or recovery with simultaneous power generation.

Keywords: energy generation; nutrient recovery; nutrient removal; wastewater; microbial fuel cell



Citation: Paucar, N.E.; Sato, C. Microbial Fuel Cell for Energy Production, Nutrient Removal and Recovery from Wastewater: A Review. *Processes* **2021**, *9*, 1318. <https://doi.org/10.3390/pr9081318>

Academic Editors: Alazne Gutiérrez and Roberto Palos

Received: 5 July 2021
Accepted: 27 July 2021
Published: 29 July 2021

Publisher's Note: MDPI stays neutral with regard to jurisdictional claims in published maps and institutional affiliations.



Copyright: © 2021 by the authors. Licensee MDPI, Basel, Switzerland. This article is an open access article distributed under the terms and conditions of the Creative Commons Attribution (CC BY) license (<https://creativecommons.org/licenses/by/4.0/>).

1. Introduction

Water, energy, and food are essential for all living forms to survive and thrive, and they are inseparably linked. Although humans have made great strides in securing those resources, the world is facing an uphill battle due largely to the increasing human population and climate change. By the next decade, the world is expected to face 40% freshwater and 36% energy shortages [1,2], together with increasing demand for food [3,4] and treatment of wastewater.

1.1. Wastewater

Currently, most conventional wastewater treatment plants (WWTPs) are energy-consuming facilities that employ energy-intensive strategies such as aeration-based heterotrophic biological treatment [5,6]. According to the Electric Power Research Institute [7], up to 3–4% of the total electricity consumed in the U.S. is related to the water management cycle, including wastewater treatment [8]. Average energy consumption in conventional WWTPs ranges from 0.2 to 0.8 kWh/m³ depending on the wastewater sources, quantity, constituent composition, process type, pollutant nature, treatment capacity, and regional differences (weather, electricity costs, etc.) [9–13].

In recent years, wastewater has been considered as a renewable resource of water [14], nutrients, and energy [14–19]. Domestic wastewater is estimated to contain 13 kJ/g of COD of chemical energy, which is nine fold more than the energy required to treat it (Heidrich et al., 2010; Yang et al., 2018). Therefore, if its energy were effectively recovered, no external energy input would be required to operate WWTPs [20,21].

1.2. Electrochemical Energy Generator/Generation

The increase of atmospheric pollution partly due to the emission of sulfur and nitrogen oxides during fuel combustions may induce irreparable damages to the earth [22,23]. To

overcome the energy and environmental crisis caused by the utilization of fossil fuels, a new energy revolution based on renewable resources is beginning to take shape, with electricity as the backbone of energy.

Theoretically, electrochemical processes can be carried out with little energy losses and, therefore, they produce minimal waste heat (heat pollution) and greenhouse gases (air pollution) [22]. Metal/air batteries, fuel cells (FCs), and redox flow batteries (RFBs) are a set of energy generators [24]. The advantages of these devices are that: (a) chemical energy is directly converted to electrical energy; (b) modular construction is possible; (c) they can be readily transported to transform electrical energy into mechanical energy (i.e., electric vehicles) [22,25,26]. Nonetheless, the requirements for the expensive catalysts are the main drawback for the oxygen cathode of metal/air batteries. Nickel-cobalt-manganese lithium batteries, for example, have relatively high energy and power density; however, the large-scale manufacture of these batteries is limited by the high price and limited sources of cobalt [24] and by the risks associated with the flammability and explosiveness of lithium-ion batteries. Furthermore, FCs and RFBs normally require ion-exchange membranes [24] with working temperatures above room temperature [22,27] and relatively high purity feed solutions [25,26], all of which increase the capital cost of the systems. Microbial fuel cells (MFCs), on the other hand, are bioelectrochemical systems capable of using wastewater as an energy source to generate electric power while improving the quality of the water environment.

1.3. Nutrients

The discharge of wastewater containing high levels of nutrients and organics to a receiving water body is a potential cause of eutrophication and hypoxia in the water environment [28,29]. Therefore, nutrients such as phosphate (PO_4^{3-}) and ammonium (NH_4^+) are being removed or recovered in WWTPs using methods that require large energy input in order to meet the discharge requirements [30].

Phosphorus (P) is essential to all forms of life and crucial to crop yields [31], and there is no substitute for it [21]. The phosphorus cycle is generally a one-way flow: all phosphorus originates from phosphate rocks and ends up in the sea as marine sediments [32]. As the world population is projected to grow to 9 billion by 2050, securing a phosphorus supply will be critical to future food security [31]. Since the commercial phosphate rock reserves are predicted to reach a critically low level within a century [33], the recovery of P from wastewater has become an emerging topic [34]. WWTPs are unexploited sources of phosphorus with an annual worldwide potential of 3 million tons of phosphate [35,36]. It is estimated that the total phosphorus available in sewage, if recovered fully, could supply about 15–20% of the global phosphorus demand [37], which can be an imaginable substitute for phosphate rock mines.

For the growing population, natural nitrogen-fixing is insufficient; thus, about half of the food production in the world is depending on synthetic fertilizer [38]. Nitrogen (N) used in producing fertilizer is predominantly manufactured using the industrial Haber-Bosch process [21] in which atmospheric nitrogen (N_2) is converted to ammonia (NH_3) [39]:



Because this reaction requires high temperature and pressure, the manufacturing process is energy-intensive. Furthermore, H_2 is generally derived from nonrenewable fossil sources, and greenhouse gases (e.g., CO_2) are released into the atmosphere [21]. High levels of NH_4^+ -N concentrations are commonly present in textile, fertilizer, petrochemical, and pharmaceutical industrial wastewater [40]. For instance, ammonium content in municipal wastewater is ~100 mg/L [41], ~9000 mg/L in human urine [42], ~8100 mg/L after urine hydrolysis [43], and ~2000 mg/L in landfill leachate [44]. Annually, domestic wastewater contributes 20 million tons of ammonium, which corresponds to ~19% of the annual ammonium production by the Haber-Bosch process [45]. By 2050, it is projected that the ammonium in domestic wastewater will further increase to 35 million tons annually [45].

In a conventional wastewater treatment system, ammonium is removed by methods that require a large amount of energy (i.e., nitrification and denitrification methods), in which the aeration for nitrification alone involves around 50% of the total energy used in the wastewater system [46] and around 60% of its operational cost [47]. Technologies that do not require intensive aeration and are able to recover valuable resources are attractive.

In recent years, MFCs have been studied to remove or recover nutrients from wastewater together with the generation of power in a sustainable way [16,19,28,48]. Because phosphorus (P) and nitrogen (N) are principal ingredients of fertilizer, the recovery of P and N increases the economic feasibility of the treatment system [49].

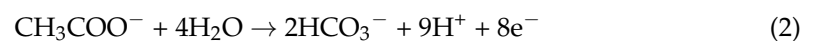
Although past research has focused on the removal of nutrients, recovery is now becoming recognized as a cost-effective way to treat wastewater [50]. The choice between removal and recovery of nutrients depends on their relative concentrations in wastewater. Removal may be more applicable to low concentration streams, while the recovery may be a better approach for high concentration waste streams such as activated sludge, animal waste, and landfill leachate [50]. Effluent and sludge from an anaerobic digester (i.e., digestate) contain high levels of organics, NH_4^+ , PO_4^{3-} , and other constituents [51]. The recovery of nutrients, mainly N and P, from wastewater for use in agricultural practices contribute to sustainable wastewater management [18,19,52].

This paper provides a review of MFC technologies applied to the removal and/or recovery of P and N, organics (as COD), and bioenergy (as electricity) from various wastewaters. The aim of this review is to provide the current perspective on MFCs, focusing on the recent advancements in the areas of nutrient removal/recovery and power generation. To the best of the authors' knowledge, there is no similar review related to these specific topics.

2. Microbial Fuel Cell

Microbial fuel cells (MFCs) are ecofriendly biotechnologies in which electrogenic or electroactive bacteria (EAB) convert chemical energy contained in their substrates to electricity [9,21,53–55]. Thus, MFCs have the potential to provide sustainable wastewater treatment with a low carbon footprint [56]. An MFC consists of an anode, cathode, microorganism, substrate (anolyte), and conductive wire (external circuit). A conventional dual-chamber (or two-chamber) MFC consists of an anode and cathode chambers (or compartments) that are separated by a cation exchange membrane (CEM), also known as a proton exchange membrane (PEM) [18,57]. Various types of separators have been used for MFCs such as canvas [58]; microporous filtration membranes [59], nylon-infused membrane [60], carbon paper [61], Nafion™ [62], Ultrex™ [63], and ceramics [64–66].

In the anode chamber, the EAB is responsible for the generation of electrons and protons [67–69]. The reaction is typically represented by the oxidation of acetate [68]:



The EAB act as a biocatalyst for the oxidation of substrate and transferring electrons to the anode [70–72]. Microscopic observations have revealed that EAB proliferates over the anode surface to form a multi-layered biofilm [73,74]. The EAB in the monolayer biofilm that is in direct contact with the anode typically utilizes outer-membrane redox proteins and cytochrome cascades to transfer electrons directly to the anode [75]. On the other hand, the microbes in the outer layers develop nanowire structures to connect with the anode surface or use other microbes via an extracellular conductive matrix to transfer electrons, known as interspecies electron transfer [76,77]. In addition to the direct electron transfer, the indirect transfer can also occur via soluble electron shuttles or mediators that transfer extracellular electrons to the anode [78,79]. Based on electron transfer mediators, MFCs can be divided into mediator and non-mediator (or mediator-less) microbial fuel cells. There are two main types of mediators added to microbial fuel cells. The first category is synthetic mediators, mainly dye-based substances, such as phenazine, phenothiazine, indophenol, and thionine [80]. The second type is those synthesized by microorganisms

and used by the same organisms or by other organisms for transferring electrons. For instance, *Pseudomonas aeruginosa* strain KRP1 synthesizes mediator substances such as pyocyanin and phenazine-1-carboxamide [81].

Electrons produced in the anode chamber flow through the external circuit to the cathode, generating a current [53,72,82,83].

The cathode chamber contains electron acceptors (e.g., O₂) to facilitate reduction reactions, typically given as [84]:



While electrons flow through the external circuit, protons pass through the PEM to react with oxygen to form water molecules in the cathode chamber [67,69]:



Given the facts that domestic, agricultural, and industrial wastewaters contain various substrates that can serve as a renewable fuel source for MFCs [85,86] and that MFCs have the potential ability to capture a large fraction of chemical energy from wastewater [9,21], MFCs can be self-sustaining wastewater treatment technologies that require no external power sources [87]. Specifically, as compared to the conventional wastewater treatment, the MFC technology offers the following potential advantages:

- (a) Energy-saving—MFCs require no or reduced aeration [88–94];
- (b) Production of less sludge [89,94–98]—MFCs produce less sludge compared to the conventional activated sludge processes [90,91] or even anaerobic digestion processes [88,92,93]. In an MFC, a large fraction of the organic mass in wastewater is converted to electrical energy at a high conversion efficiency [90–94,97,99] with faster reaction kinetics [89];
- (c) No generation of harmful toxic byproducts [100,101] such as trihalomethanes (THMs) produced in the chlorination of wastewater [102];
- (d) Ability to recover valuable products from wastewater; i.e., electricity [94,97,99] and nutrients [20,28,49,103];
- (e) Easy operation under the different conditions [100] such as various temperatures [90] even at low temperatures [88,92,93], various pH values, and with diverse biomass [90];
- (f) Clean and efficient technology [100,101]. MFCs can produce electricity with less environmental burdens and a low carbon footprint [56,88,96].

On the other hand, the present MFC technology possesses some disadvantages including, but not limited to [101,104]:

- (a) Low power output;
- (b) Expensive construction materials; e.g., platinum for an electrode;
- (c) Difficulty to scale up to meet the capabilities for industrial needs.

Despite the inherent limitations of MFC technology, overall, it possesses several advantages over conventional wastewater treatment methods, and thus, it is gaining recognition as a potential sustainable wastewater treatment technology. The new advanced electrode materials such as 2D nanomaterials are expected to promote the development of electromicrobiology [101].

3. Energy Generation by MFCs

Energy scarcity and water pollution are two important challenges that the planet Earth is facing today [105]. The MFC technology may provide a partial solution to these challenges.

The efficacy of MFCs depends on a number of biological, physicochemical, and electrochemical factors, and operational parameters. The performance (in terms of electricity generation) of the different types of MFCs with various wastewaters and operational conditions are summarized in Table 1.

The typical biological factors are the types, numbers, and catalytic activity of the microorganisms in the MFC. The energy losses at the anode can be attributed to the loss of electrochemical activity of the microorganisms [106] and the anode overpotential transport loss [107]. The physicochemical and electrochemical factors include, but are not limited to, the types and effective surface area of the electrode, electrolytic resistance [101], rate of the proton transport through the PEM, rate of the reduction reaction at the cathode [89,108], and external resistance applied across the electrodes [109–111]. The organic loading rates [21,48,112,113], and type and concentration of the substrate are the operational parameters. The intricate interdependence of these factors and parameters makes the optimization of the MFC difficult. For instance, the rate of substrate conversion can be affected by the total amount of electroactive bacterial cells, a phenomenon of mixing mass transfer, bacterial growth kinetics [114–116], organic loading rate per biomass (grams of substrate per gram of biomass per day), transmembrane efficiency for the proton transport [117], and total potential of the MFC [114,118].

Internal resistance is one of the major electrochemical factors that affect MFC performance. The internal resistance can be divided into ohmic resistance, charge transfer resistance, and diffusion resistance [119,120]. The ohmic losses occur due to the resistances of the electrodes, PEM, and electrolytes [121]. On the other hand, the charge transfer and diffusion resistance take place in the interface between the electrodes and the surrounding electrolyte [122,123]. The power generation in an MFC is affected by the surface area of the PEM [124]. If the surface area of the PEM is smaller than that of the electrodes (anode and cathode), the internal resistance of the MFC will increase to limit power output [121]. Internal resistance is also a function of the distance between the cathode and anode. For the optimal design, the anode and cathode should be situated as close as possible.

To evaluate the MFC performance, cost-effectiveness must be considered. In a double-chamber MFC, PEM plays an essential role in the MFC performance, and also affects the operation and maintenance costs. Many of the past studies on MFCs used commercial Nafion as PEM. Nafion-membrane is highly sensitive to wastewater contaminants (e.g., ammonium). UltrexTM, a cation exchange membrane, provides more stability but has a larger resistance and less ion selectivity than Nafion [63]. Carbon paper (as a separator) can reduce internal resistance and the cost of the MFCs, yet presently there is no credible data on the stability of this material for an extended period of time.

Ceramic materials have been demonstrated to be a suitable replacement for commonly used membranes [66]. Ceramics are less expensive than the PEMs and offer high stability and better conditions for the growth of exoelectrogenic microorganisms [64–66]. Thus, ceramic can improve MFC power output and treatment efficiency. Despite these benefits, the loss of anolyte through evaporation can be one of the critical challenges. More investigations are needed to address the challenges of the different materials to improve the MFC performance and cost-effectiveness.

3.1. Coulombic Efficiency (CE)

The substrate is also an important factor for electricity generation, as it serves as a source of energy for the microorganisms, thus for the MFC [125]. To enhance MFC's performance, the substrate needs to be oxidized efficiently [126]. The efficiency of electron recovery can be measured by the Coulombic efficiency (CE). The CE represents the fraction (in %) of electrons that are recovered (as current) from the substrate [53]. In other words, the CE is the fraction of electrons that are liberated from the substrate and transferred to the anode electrode [127]. The CE usually depends on the type of microorganisms and substrates, duration of the experiment, and design of the MFCs [128]. Researchers found lower CE values (e.g., 14%) when treating real wastewater [127]. The current density and CE values achieved by a batch or fed-batch MFC system are typically low [128–130]. The low CE values typically indicate that the exoelectrogens (that form the biofilm) are using more of the energy extracted from the substrate for biosynthesis rather than electricity generation [127]. In order for the CE to increase, the influent substrate concentration

must decrease and anode potential should increase [128]. Methanogens, which reduce the CE, should be eliminated from the system. More research is required to understand the interactions between biofilm growth and the electrochemical processes [131]. Optimized external resistance generates a selective pressure inside the anode chamber, favoring the growth of exoelectrogenic microorganisms, therefore, increasing the CE of the MFC [132].

Marzorati et al. [133] used lignocellulosic materials including giant canes (GC) and maize stalks (MS) to construct two different natural cylindrical-shaped air-cathode MFCs. The GC and MS acted as separators in the GC-MFC and MS-MFC dual-chamber MFCs. The MFCs were fed swine manure with a cyclical addition of sodium acetate and were monitored for the 20-day acclimation period and 3 feed cycles. During the feed cycles 1 and 2, the maximum power density and CE were slightly increased from 43 to 44 mWm^{-2} and 13% to 18%, respectively, in the GC-MFC, and from 29 to 33 mWm^{-2} and 12% to 15%, respectively, in the MS-MFC. In feed cycle 3, the power density and CE of the MS-MFC were 32 mWm^{-2} and 20%, respectively, and higher than those of the GC-MFC (i.e., 20 mWm^{-2} and 4%, respectively). The GC-MFC showed a considerable drop of the CE in feed cycle 3 compared to that in cycles 1 and 2 [133].

3.2. Effect of Organic Loading Rate (OLR)

In general, MFCs can achieve higher CEs than other electricity-generating devices, and the CE decreases with increasing organic loading rate (OLR) [48,103,128]. Ye et al. [21] obtained the maximum CE of about 25% and the maximum voltage of 598.9 mV at the OLR of 435 mg COD/L d, whereas they observed the CE of 2.21% and the voltage of ~480 mV at 870 mg COD/L d. Similarly, in a study by Di Lorenzo et al. [112], the CE decreased from $68 \pm 7.2\%$ to $49 \pm 2.7\%$ when the OLR was increased from 16 to 161 kg COD/ m^3 d. Mansoorian et al. [48] generated bioelectricity using a catalyst-less and mediator-less membrane dual-chamber MFC, which was fed dairy wastewater. Their MFC produced the CE of ~15%, and the maximum power density of 621.13 mW/m^2 of the anode surface at the OLR of 53.22 kg COD/ m^3 d, and the maximum CE of 37.16% and the maximum power density of ~200 mW/m^2 at 17.74 kg COD/ m^3 d. The lower CE at the higher OLR may be explained by the following: (a) the non-exoelectrogen microbes (heterotrophs, methanogens) are more active than the electrochemically active microbes [21,134]; and (b) substrate may be used for the microbial growth instead of using for the conversion of the substrate to electricity [48,135,136].

In a dual-chamber MFC, the higher COD loading to the anode chamber can lead to membrane fouling adversely affecting its performance [137]. In contrast, lower COD loadings could facilitate higher electricity generation [113,138]. It has also been found that at low OLRs, MFCs require more time to reach their maximum performance (i.e., maximum current density and maximum power density) [139]. The Coulombic efficiency can be optimized by improving the electrode surface area per reactor volume [97,104].

3.3. Effects of Hydraulic Retention Time (HRT)

The hydraulic retention time (HRT) poses direct effects on the types and abundance of the microbial community in the MFC system [69,140]. In a study with a catalyst-less, mediator-less dual-chamber MFC, Mansoorian et al. [48] treated dairy industry wastewater with the HRT ranging from 2 to 8 d. They reported the maximum power density of 621.13 mW/m^2 of the anode surface at the HRT of 5 d. In treating synthetic municipal wastewater using the dual-chamber MFC, Ye et al. [19] found that the maximum power density decreased from 253.84 mW/m^2 to ~200 mW/m^2 of the anode surface as the HRT decreased from 0.69 to 0.35 d. This may be due to the fact that the high flow rate might have caused incomplete mixing of the feed substrate solution [140]. The increase of the HRT from 3 to 5 days promoted the longer contact time between the biofilm and the organic substrate in the MFC improving the substrate degradation, electron production, and transport, thus increasing voltage [48]. In the dual-chamber MFC treating synthetic wastewater, with the HRT ranging between 0.35 and 0.69 d, the changes in the COD removal and nutrient

recovery efficiencies were insignificant, provided >92% COD removal and about 80–90% nutrient recovery efficiency [19]. In addition, in the dual-chamber MFC, the HRT affected the generation of electricity but its effect on the nutrient recovery (from synthetic municipal wastewater) was insignificant [49]. While the HRT affects energy generation, its effect on nutrient recovery from synthetic wastewater appeared negligible.

Mansoorian et al. [48] studied treated dairy industry wastewater by varying the HRT from 2 to 8 d; however, nutrient recovery was not affected by HRT. They reported the maximum removal efficiencies of 90.46% for COD, 69.43% for $\text{NH}_4^+\text{-N}$, and 72.45% for P in suspended solids at ~30 days, and 31.18% for dissolved P at ~6 days.

3.4. Effects of Ammonium Concentration

An excess of NH_4^+ in the feed solution negatively affects the generation of electricity. Ryu et al. [141] used a dual-chamber MFC to treat piggery wastewater and observed that the cathode potential decreased from ~0.8 to ~0.5 V when an ammonium concentration in the anode chamber increased from 30 to 100 mg/L. The most likely explanation for the decrease in potential is that nitrifying microbes compete for the electron acceptor (i.e., O_2) on the cathode electrode. In a study by Ye et al. [49], a dual-chamber MFC was operated in a continuous mode with the influent ammonium concentrations ranging from 5 to 40 mg/L as N ($\text{NH}_4^+\text{-N}$). They observed the maximum power density of 230.17 mW/m^2 of the anode surface on average at the influent $\text{NH}_4^+\text{-N}$ concentration of 5 mg/L; however, the power density decreased by approximately 50% (to ~120 mW/m^2) when the $\text{NH}_4^+\text{-N}$ concentration was increased to 40 mg/L. The CE also decreased from 25% (at maximum) to 15% when the influent $\text{NH}_4^+\text{-N}$ concentration was increased from 5 to 40 mg/L [49]. Similar results were reported by other researchers [113,142,143]. Ye et al. [49] also reported that the COD removal efficiency was above 85% with the $\text{NH}_4^+\text{-N}$ concentrations between 5 and 40 mg/L. At the same $\text{NH}_4^+\text{-N}$ concentration range, the P removal/recovery was in a range from 11.37% to 13.33% in the anode chamber and the P recovery was 76.03 to 83.23% in the cathode chamber. On the other hand, the $\text{NH}_4^+\text{-N}$ recovery fell from 85.11% to 15.33% when the $\text{NH}_4^+\text{-N}$ concentration was increased from 5 to 40 mg/L. The results suggest that NH_4^+ cannot be effectively recovered from ammonium-rich wastewater in dual-chamber MFCs.

3.5. Effects of Dissolved Oxygen Concentration

The dissolved oxygen (DO) in the cathode chamber affects the generation of electricity; thus, it is important to maintain an optimal DO to obtain the maximum performance of MFCs [144]. Past researchers have shown that an increase in DO in the cathode chamber increased the generation of current [103,145]. In a study with a dual-chamber MFC treating synthetic wastewater, Tao et al. [144] observed that an average CE decreased from 52.48 to 23.09% when DO decreased from 3.5 to 2 mg/L in the cathode chamber. The decrease of the CE may be due to the increase of electrochemically inactive microorganisms in the anode chamber and/or the increase of the internal resistance when DO decreased in the cathode chamber. The power density also decreased from 530 mW/m^2 to 178 mW/m^2 when DO decreased in the cathode chamber from 3.5 mg/L to 2 mg/L DO [144]. Tao et al. [144] also found that 2.0 mg/L DO in the cathode chamber was sufficient for the P and N removal. At this O_2 level, the chemical precipitation and biological absorption provided a total P removal of 80%. Adjusting DO to its optimal level can therefore favor the power generation, CE, and removal of N and P.

3.6. Effects of Temperature

In general, the microbial activity increases as temperature increases, thus electricity generation can be boosted by raising the temperature [146,147]. However, the long-term exposure of microbes to high temperatures may damage the cells (e.g., nucleic acid, cell function) resulting in a dramatic decline of voltage and current [48]. Firdous et al. [147] treated wastewater from a vegetable oil industry using a dual-chamber MFC and found

that the increasing temperature from 25 to 35 °C resulted in an increase of the CE from 33% to 36.5%, the current from 4.05 to 11.72 mA, and the power density from 2166 to 6119 mW/m². The higher temperature also enhanced the COD removal (80–90%) due to the increase in the population of mesophilic microorganisms in the anode chamber [147]. The COD removal ranged from 40% to 80% at 25 °C and from 60 to 90% at 35 °C; and the P removal efficiencies were 56.9% and 73.6% at 25 °C and 35 °C, respectively [147]. The optimum temperature for mesophilic microbes is in a range between 35 °C to 40 °C [148]. Warmer temperatures, in general, have positive effects on the power generation, CE, and removal of organics (COD) and phosphorus.

3.7. Effects of Resistance

In an MFC, the external resistance regulates the flow of electrons and consequently regulates the power generation efficiency. In other words, the lower resistance facilitates the electron flow from the anode to the cathode, supporting the microbial electron respiration on the anode, thus enhances the substrate removal efficiency [48,110]. On the other hand, the higher resistance reduces electron flow towards the cathode maintaining a high potential difference, thus enhances the power harvest [109,111,149]. The low voltage at a high external resistance may be due to the slower speed of electrons used on the cathode, compared to its transfer rate [48]. The maximum power density is achieved when the internal and external resistances are equal [128,150]. Various factors such as the distance between the electrodes, electrode material, ionic strength of the anolyte and catholyte, substrate properties, operation modes, and MFC design affect the internal resistance of MFCs. The optimization of these factors can improve the MFC performance. In general, a single-chamber MFC exhibits lower internal resistance than the dual-chamber MFC: such information should be taken into consideration when designing MFC systems [119].

4. Nutrient Removal and Recovery

4.1. Nutrient Removal

The removal of nutrients from the WWTP effluent can reduce the eutrophication potential in the receiving water environment. In comparison with energy-intensive nutrient removal technologies currently employed in the conventional WWTPs, MFCs have the advantage that they generate electricity. The effectiveness of different types of MFCs for the removal and/or recovery of nutrients from various wastewaters and operational conditions are summarized in Table 2.

Table 1. Energy production in MFC systems from different types of wastewater and different operational conditions.

Type of Wastewater	MFC Type/Operation Mode	MFC Operation Specifications	Electrodes Specifications	External Resistance/Wired	Maximum Voltage	Power Density	Current Density	Coulombic Efficiency	Reference
Synthetic wastewater	Mediator-less dual chamber MFC 2-stage feed-batch mode (Two sets of dual-chamber H-type bottles, operated for 120 days).	At 20 °C Anode influent pH > 8 MFC volume: 300 mL Nafion membrane separation. Cathode chamber continuously aerated using an aquarium pump.	Anode: plain carbon cloth. Cathode: Pt catalyst (0.5 mg/cm ² 10% Pt on carbon cloth electrode).	1000 Ω initial stage then 430 Ω at maximum power. Electrodes connected with a titanium wire (0.5 mm, purity > 99.98%).	−550 ± 10 mV	72 mW/m ²	62 mA/m ²	10%	[103]
Primary effluent of municipal wastewater	200 L Modularized MFC system (96 tubular MFC modules of 2 L/each). Continuous mode, operated for one-year.	At ~10–28 °C Cation exchange membrane (CMI-7000). Volume of each MFC: 2 L Catholyte recirculated by a submersible pump.	Anode: carbon brush. Cathode: carbon cloth coated with nitrogen doped activated carbon powder.	15 Ω Wired with titanium wire.	—————	~200 mW	~50–150 mA	—————	[16]
Dairy industrial wastewater	Catalyst-less and mediator-less membrane dual chamber MFC Continuous mode.	At 35 °C Anode influent pH: 8.5–10.3. HRT = 5 days MFC volume: 2 L Proton exchange membrane (Nafion 117). Cathode chamber continuously aerated using an aquarium pump (2 mg/h).	Anode and cathode electrodes made from graphite plate (14 × 6 × 0.5 cm ³).	1 kΩ Electrodes connected with copper wire (2 mm diameter and 35 cm length).	0.856 V	621.13 mW/m ²	3.74 mA	6% 37%	[48]
Untreated human urine	3-stage MFC system in a continuous mode (System of MFCs that fits urinals).	At 22 ± 2 °C MFC volume: 6.25 mL anode chamber and open-to-air cathodes. cation exchange membrane (CMI-7000, 25 mm diameter)	Anode: Plain fiber veil electrodes with 12 layers of 4.18 cm ² (width of 2.2 cm and length of 1.9 cm). Cathode: hot-pressed activated carbon onto carbon fiber veil (4.9 cm ²).	1 kΩ Wired with Nickel-chromium wire (0.45 mm thickness).	—————	1st stage: 14.32 W/m ³ (Absolute power: 358 μW) 3rd stage: 11.76 W/m ³ (Absolute power: 294 μW)	—————	—————	[28]
Domestic wastewater	Algal biofilm MFC. Continuous mode.	At 25 ± 1 °C MFC volume: 1.6 L Prepared microalgal biofilm fixed at the middle of the cylindrical MFC. Continuous irradiation (135 μmol m ^{−3} s ^{−1}).	Anode and cathode electrodes made of piece of carbon cloth (diameter 90 mm and thickness 8 mm) interwoven with titanium wire. Anode placed in lower chamber of the MFC and cathode placed on the water surface.	1 kΩ	After start up: 580 mV Steady value: 270 mV Batch mode: 566 mV	0.094 kW/m ³ Batch mode: 62.93 mW/m ²	—————	* Batch mode: 17.01%	[20]

Table 1. Cont.

Type of Wastewater	MFC Type/Operation Mode	MFC Operation Specifications	Electrodes Specifications	External Resistance/Wired	Maximum Voltage	Power Density	Current Density	Coulombic Efficiency	Reference
Effluent drain of vegetable oil industry	Dual chambered MFC. Batch mode.	At 35 °C Anode influent pH = 5.7 HRT = 72 h. MFC volume: 500 mL Proton exchange membrane (CMI-7000)	Anode: titanium rod. Cathode: carbon cloth	1 kΩ	5839 mV 5685 mV at 25 °C	6119 mW/m ² 2166 mW/m ² at 25 °C	11.72 mA 4.05 mA at 25 °C	36.5% 33% at 25 °C	[147]
Swine manure and sodium acetate	Air-cathode MFC Giant canes (GC-MFC) and Maize stalks (MS-MFC). Batch mode.	At 25 ± 1 °C GC and MS external diameter: 2.5 cm and 10 cm length. Initial analyte COD: 10.3 g/L and 3 g/L sodium acetate added to anodic chamber.	Anode: plain carbon cloth (7.8 × 10 cm) Cathode: carbon cloth (6.6 × 10 cm) with surface treatment (microporous layer) by mixing carbon black particles, PTFE solution, distilled water, and a non-ionic surfactant.	100 Ω Wired with plastic-insulated copper wire. Internal resistance: ~60 for GC-MFC and 80–95 Ω for MS-MFC.	GC-MFC Cycle 1: ~500 mV Cycle 2: ~450 mV Cycle 3: ~5 mV MS-MFC Cycle 1, 2, & 3: ~450 mV	GC-MFC Cycles 1 & 2: 43–44 mW/m ² Cycle 3: 20 mW/m ² MS-MFC Cycles 1 & 2: 29–33 mW/m ² Cycle 3: 32 mW/m ²	GC-MFC (mA/m ²): Cycle 1: 212 Cycle 2: 227 Cycle 3: 30 MS-MFC (mA/m ²): Cycle 1: 167 Cycle 2: 197 Cycle 3: 227	GC-MFC: Cycle 1: 13% Cycle 2: 18% Cycle 3: 4% MS-MFC: Cycle 1: 12% Cycle 2: 15% Cycle 3: 20%	[133]
Digestate coming from an anaerobic digester	MET (MFC or MEC) coupled with struvite crystallization Single chamber, air-cathode MFC batch mode.	At 23 ± 1 °C MFC volume: 28 mL pH adjusted to 8.5 with NaOH (1 mol/L)	Anode: graphite fiber brush (with a core of titanium wires). Cathode: carbon cloth (30 wt.%) with platinum catalyst (0.4 mg Pt/cm ²) on the liquid-facing side and four PTFE diffusion layers added on the air-facing side.	1 kΩ	0.50 ± 0.01 V	14.19 ± 0.15 W/m ³ 0.43 W/m ²	1.56 A/m ²	35.04 ± 0.2%	[151]
Pre-hydrolyzed human urine	Electrodialysis system embedded in an MFC. Continuous mode.	Anode and cathode chambers separated by a recovery chamber (each chamber 200 cm ³). Cation exchange membrane (CMI-7000) between anode and recovery chamber. Anion exchange membrane (AMI-7000) between recovery and cathode chamber. Peristaltic pump for feed (0.5 L/d).	Anode: graphite granules (2–5 mm diameter) and two graphite rods (5 mm diameter, 9.5 cm length) for current collector. Cathode: carbon cloth (20 × 5 cm) with carbon-based catalyst on the inner side, four PTFE diffusion layers on the outer side and titanium mesh for current collector.	—————	—————	—————	3 A/m ²	—————	[15]

Table 1. Cont.

Type of Wastewater	MFC Type/Operation Mode	MFC Operation Specifications	Electrodes Specifications	External Resistance/Wired	Maximum Voltage	Power Density	Current Density	Coulombic Efficiency	Reference
Synthetic domestic wastewater	Photoautotrophic H-type MFC. Continuous mode.	At 25 ± 3 °C MFC volume: 400 mL (each chamber). Cathodic chamber mechanically aerated (DO of ~ 6.5 mg/L). Nafion 117 proton exchange membrane (8.5 cm ²).	Anode and cathode electrodes made of carbon brushes (7.5 cm in length, 4 cm in diameter) pretreated by acid soaking and heating (450 °C, 30 min).	500 Ω Wired with copper wire.	~ 460 mV	466.9 ± 24.4 mW/m ³	~ 0.6 mA	3.3–3.9%	[152]
Synthetic domestic wastewater	Double-chamber MFC. Continuous mode.	At 24 ± 2 °C pH = 7 ± 0.15 MFC volume: 350 mL (each chamber). Peristaltic pump for anolyte feed (0.35 mL/min). Cathodic chamber mechanically aerated (DO of 6 mg/L). Proton exchange membrane (CMI-7000).	Anode: graphite felt in cylinder-shaped form (diameter 30 mm, thickness 60 mm). Cathode: carbon-fiber brush (3 cm length, 3 cm diameter) coated with titanium bar.	1 k Ω Wired with copper wire.	598.9 mV at OLR of 435 mgCOD/L.d. ~ 475 mV at OLR of 870 mgCOD/L.d.	253.84 mW/m ² at OLR of 435 mgCOD/L.d. ~ 170 mW/m ² at OLR of 870 mgCOD/L.d.	—————	25.01% at OLR of 435 mgCOD/L.d. 2.21% at OLR of 870 mgCOD/L.d.	[21]
Synthetic municipal wastewater	Double-compartment MFC. Continuous mode.	At 22 ± 2 °C MFC volume: 305 mL (each chamber). Peristaltic pump for anolyte feed (0.35 mL/min). Proton exchange membrane (CMI-7000).	Anode: graphite felt in cylinder-shaped form (diameter 30 mm, thickness 6 mm). Cathode: carbon-fiber brush (30 mm length, 30 mm diameter).	1 k Ω Wired with copper wire.	598.9 mV at 5 mg.NH ₄ ⁺ -N/L. ~ 425 mV at 40 mg.NH ₄ ⁺ -N/L.	230.17 mW/m ² at 5 mg.NH ₄ ⁺ -N/L. ~ 120 mW/m ² at 40 mg.NH ₄ ⁺ -N/L.	—————	25% at 5 mg.NH ₄ ⁺ -N/L. 15 at 40 mg.NH ₄ ⁺ -N/L.	[49]
Synthetic urine-containing wastewater	Three-chamber resource recovery MFC. Batch mode	At 30 °C MFC volume: ~ 23 mL anode chamber, ~ 19 mL middle chamber, and ~ 19 mL cathode chamber. Cation exchange membrane (Selemion CMV) between anode chamber and middle chamber. Anion exchange membrane (Selemion AMV) between middle chamber and cathode chamber.	Anode: graphite fiber brush (2.5 cm diameter, 2.5 cm length) heated at 450 °C for 30 min. Cathode: circular activated carbon air-cathode (7 cm ²).	10 Ω * Internal resistance: 208 Ω	0.72 V	1300 mW/m ²	1.30 ± 0.30 mA	55%	[17]

Table 1. Cont.

Type of Wastewater	MFC Type/Operation Mode	MFC Operation Specifications	Electrodes Specifications	External Resistance/Wired	Maximum Voltage	Power Density	Current Density	Coulombic Efficiency	Reference
Synthetic municipal wastewater	Two-chambered MFC. Continuous mode.	At 22 ± 2 °C MFC volume: 350 mL (each chamber). Proton exchange membrane (CMI-7000). HRT: 0.69 d–0.35 d. OLR: 435–870 mg/L.d.	Anode: graphite felt in cylinder-shaped form (diameter 30 mm, thickness 6 mm). Cathode: carbon-fiber brush (30 mm length, 30 mm diameter).	1 k Ω Wired with copper wire.	598.9 mV at HRT = 0.69 d, OLR = 435 mg/L.d. ~515 mV at HRT = 0.35 d, OLR = 870 mg/L.d.	253.84 mW/m ² at HRT = 0.69 d, OLR = 435 mg/L.d. ~200 mW/m ² at HRT = 0.53 d, OLR = 870 mg/L.d.	—————	25.01% at HRT = 0.69 d, OLR = 435 mg/L.d.	[19]

4.1.1. PO_4^{3-} -P and NH_4^+ -N Removal

In a study by [153], an algal bioreactor was connected externally to an MFC to treat domestic wastewater. Their hybrid system improved the removal of total P from 58% to 92% and removed 81.9% of organics (as COD), as high as 95.5% of total N, and 96.4% of total P [20]. Wang et al. [152] studied nutrient (P and N) removal and bioenergy recovery from synthetic wastewater using an immobilized microalgal-based photoautotrophic microbial fuel cell (PMFC) system. The PMFC system achieved the removal efficiencies of 93.2% for soluble COD, 95.9% for NH_4^+ -N, and 82.7% for PO_4^{3-} -P in the anode compartment, and 27.7–50% for NH_4^+ -N and 37.1–67.9% for PO_4^{3-} -P in the cathode compartment. The reduction of nutrient levels in the cathode compartment was most likely due to the assimilation of P and N into the microalgal biomass. Although their system produced 466.9 mWm^{-3} , it consumed energy for pumping of anolyte and catholyte, illumination, and biodiesel production (e.g., microalgae harvesting, lipid extraction). The power produced accounted for 12.7–42.3% of the energy consumed, excluding the energy used for biodiesel production. Theoretically, the biodiesel from algal biomass could achieve energy neutrality and it could significantly enhance the economic benefits [152]. The work by Jiang et al. [153] and Wang et al. [152] demonstrated that the MFC combined with another technology can boost nutrient removal by exploiting microbial assimilation.

4.1.2. NH_4^+ -N Removal

Organic nitrogen present in synthetic wastewater can be removed by ammonification, nitrification, and followed by denitrification [154]. In a single-chamber MFC, the removal of NH_4^+ -N is mainly due to the volatilization of ammonia [48,155]. In a dual-chamber MFC, most of the organic nitrogen is transformed to NH_4^+ -N in the anode chamber [156], and the NH_4^+ -N removal is primarily due to the migration of NH_4^+ -N from the anode chamber to the cathode chamber through a PEM and volatilization in the cathode chamber [21,50,155]. Without volatilization, NH_4^+ -N can accumulate to a level of several grams per liter in the cathode chamber [42]. The migration of NH_4^+ -N can be considered as a proton shuttle [157]. Previous studies suggested that NH_4^+ -N can be removed by volatilization in single and double chamber MFCs.

4.2. Nutrient Recovery

4.2.1. Struvite

To date, only a few studies have been undertaken to recover nutrients using MFCs [15,17,19,21,49,133,158]. The recovery of P and N by MFCs has been accomplished mainly by the formation of struvite, $\text{NH}_4\text{MgPO}_4 \cdot 6\text{H}_2\text{O}$ [151,158–162]. Struvite has been demonstrated to be slow-release fertilizer [163] and has a commercial value [164–167].

Struvite can be formed by reacting similar molar ratios of ammonium (NH_4^+), magnesium (Mg^{2+}), phosphate (PO_4^{3-}), and six water molecules [158,161,167]:



In an MFC, the pH is higher near the cathode owing to the reaction represented by Equation (3). Since the solubility of struvite decreases at higher pH [168], struvite precipitation occurs near or on the surface of the cathode [158]. Since wastewater is a rich source of PO_4^{3-} [103], NH_4^+ , Mg^{2+} along with organic matters, the struvite precipitation has been considered as an ideal way to recover P and N from wastewater [167]. In general, the P content in the struvite is between 13% to 14% by weight [31]. To utilize struvite directly as the slow-release fertilizer [169,170], its purity is an important factor, which is dependent on the characteristics of the wastewater [165]. In a dual-chamber MFC, the recovery of P as struvite involves the reaction represented by Equation (5) [103], and P can be exclusively recovered since P is not involved in the redox reactions [50].

Ichihashi and Hirooka [158] used an air-cathode single-chamber MFC to treat swine wastewater. In their study, only 27% of P was recovered as struvite. This low recovery rate is

most likely due to pH buffering that inherently occurs in a single-chamber MFC, as protons (H^+) and hydroxide ions (OH^-) accumulate in the same region of the MFC [103,171]. In a study by Hirooka and Ichihashi [160], after removing the precipitates from the cathode electrode, the MFC performance was restored to almost its original level. It is most likely that the struvite precipitation at the cathode obstructed the mass transfer of ions and oxygen [160].

In a dual-chamber MFC, nutrient removal usually occurs in the anode chamber and recovery in the cathode chamber [21,49,152]. Almatouq & Babatunde [103] investigated the P recovery and electricity generation using a two-stage, mediator-less dual-chamber MFC system, which was operated in a fed-batch mode. In the first cycle, synthetic wastewater was fed to the anode chamber to remove organics (measured as COD). At the end of the first cycle, the effluent from the anode chamber was filtered and fed to the cathode chamber to recover P as struvite. In their study, 8 mM of NH_4Cl and 8 mM of $MgCl_2$ solutions were added to the cathode chamber at a rate of 6 mL/day. When the COD concentration was increased from 0.7 to 1.5 g/L, the P recovery efficiency increased from 7% to as high as 38%. The reported power density is 72 mW/m² [103]. The COD concentration and aeration rate were shown to be the key factors that affect the P recovery and electricity generation. Since the dual-chamber MFC creates an alkaline environment around the cathode, it provides better nutrient recovery efficiencies [50].

4.2.2. Precipitation of P and N with Magnesium Chloride and Seawater Bitterns (SWB)

In a study by Sciarria et al. [151], a single-chamber, air-cathode MFC was coupled with a microbial electrolysis cell (MEC) to treat digested sludge from an anaerobic digester. This MFC system removed $44.7 \pm 1.6\%$ of total COD, $35.8 \pm 1.2\%$ of PO_4^{3-} , and $10.1 \pm 0.5\%$ of NH_4^+ . Crystallized P was found at the cathode. Magnesium chloride ($MgCl_2 \cdot 6H_2O$) or seawater bitterns (SWB) were added to the effluent of the MFC to boost further precipitation of P and N. The addition of magnesium chloride resulted in $83.1 \pm 3.7\%$ reduction of PO_4^{3-} and $14.7 \pm 0.6\%$ reduction of NH_4^+ . The addition of SWB resulted in slightly higher removal of PO_4^{3-} ($87.7 \pm 2.85\%$) but there was about the same level of removal of NH_4^+ ($14.7 \pm 0.5\%$). On the other hand, the MEC led to the removal of approximately 21–30% of PO_4^{3-} and approximately 27–40% of COD before precipitation. In their experiment, the effluent of the MEC was also treated with magnesium chloride or seawater bitter to allow further nutrient precipitation. With the addition of magnesium chloride, the removals were in a range from ~68% to 74% for PO_4^{3-} and ~7% to 9% for NH_4^+ . With seawater bitterns, the precipitations of PO_4^{3-} were slightly higher, (~67–75%), while NH_4^+ removal was between ~14% and 8%. The result indicated that the MFC was 10% to 15% more efficient than the MEC in terms of the P removal. Moreover, seawater bitterns achieved better removal of PO_4^{3-} than the more expensive magnesium chloride [151]. The results suggest that, in treating wastewater containing an insufficient amount of magnesium, the addition of less expensive precipitant aids (SWB) can improve the recovery of P and N from the wastewater.

4.2.3. Effect of Organic Loading Rate (OLR) on P/N Recovery

The organic loading rate (OLR) plays an important role in nutrient removal/recovery and electricity generation. The OLR affects the microbe's metabolic activities, growth, and substrate utilization, and thus nutrient recovery and electricity generation. In a study by Hamza et al. [172], high OLRs negatively affected the generation of electricity but improved nutrient removal/recovery. Ye et al. [21] used a dual-chamber MFC to treat synthetic domestic wastewater with varying COD loading rates from 435 to 870 mg COD/L.d. In their work, they obtained the COD removal of 90% on average. When the COD loading rate was increased from 435 to 870 mg COD/L d, the NH_4^+ -N removal efficiency increased from 14% to 75.13% and the PO_4^{3-} -P removal from 12.43% to 71.5%. Note that the nutrient recovery efficiency declined in the cathode chamber because the concentrations of NH_4^+ -N and PO_4^{3-} -P were lower in the cathode chamber as a large fraction of the nutrients were

already removed in the anode chamber. In terms of the nutrient recovery, the $\text{NH}_4^+\text{-N}$ recovery efficiency was 85.11% at the loading rate of 435 mg COD/L.d and decreased to 24.34% at 870 mg COD/L.d. The $\text{PO}_4^{3-}\text{-P}$ recovery efficiency was 83.23% at the loading rate of 435 mg COD/L.d and decreased to 24.4% at 870 mg COD/L.d [21]. Thus, the P and N recovery efficiency were decreased with increasing OLR. The results suggest that the removal efficiency of organic matter (COD) and Coulombic Efficiency (CE) can be improved by feeding wastewater at low OLRs.

4.2.4. Nutrient Recovery from URINE

Human urine typically contains 9 g of $\text{NH}_4^+\text{-N/L}$, 0.7 g of $\text{PO}_4^{3-}\text{-P/L}$, and other constituents, and has been used as an electrolyte in an MFC for nutrient recovery system [42,43]. In a study by You et al. [28] nutrients were recovered from human urine in a form of struvite, while generating electricity, using a 3-stage single-chamber MFC/struvite extraction system. The first and third stage MFCs generated 14.32 W/m³ and 11.76 W/m³ of power, respectively. The second stage MFC was used for nutrient recovery. The hydrolysis reaction of urea was accelerated in the first stage. In the second stage, magnesium was added to form struvite. In the third stage, after the completion of struvite precipitation, the supernatant was treated for additional power generation and COD removal. In their work, 78% of $\text{PO}_4^{3-}\text{-P}$ and 7% of $\text{NH}_4^+\text{-N}$ were recovered as struvite. Overall, 82% of $\text{PO}_4^{3-}\text{-P}$ and 20% of COD were removed from human urine. Lu et al. (2019) developed a three-chamber MFC (called a recovery resource MFC or RRMFC) and used it to remove organics and salts, simultaneously recovering nutrients from synthetic wastewater containing urine. The RRMFC consisted of three chambers (anode, middle-recovery, and cathode chambers), and was operated in a batch mode for 33 cycles (~3 days per cycle). Synthetic urine wastewater was fed to the anode chamber where organics were oxidized, and urine was hydrolyzed. Deionized water was fed to the middle chamber where PO_4^{3-} and NH_4^+ were precipitated as struvite. The effluent of the anode chamber was fed to the cathode chamber for power generation. In their system, the removal efficiencies of COD, NH_4^+ , total N, and PO_4^{3-} reached 97%, 40%, 98%, and 99%, respectively. At the same time, the RRMFC recovered 42% of total N and 37% of PO_4^{3-} in the middle chamber. The NH_4^+ mass increased from 0 to 9.01 ± 2.12 mg in the middle chamber, indicating that a large amount of NH_4^+ migrated from the anode chamber to the middle chamber through the PEM. Similarly, PO_4^{3-} migrated from the cathode chamber to the middle chamber with the effect of the electric field. The decrease of the PO_4^{3-} concentration in the cathode chamber may be due to struvite precipitation under the alkali conditions [17]. A fraction of PO_4^{3-} may also be removed by microbial assimilation in the anode chamber [173]. The RRMFC produced the maximum currents of 1.30 ± 0.30 mA and maximum power density of 1300 mW/m² of the anode surface at an external resistance of 10 Ω . The RRMFC did not require any external energy input for its operation (Lu et al., 2019). Freguia et al. [15] used an MFC/electrodialysis-hybrid system for nutrient recovery from human urine. The fresh urine was left to hydrolyze before the supernatant was collected and used as a feed to the microbial electro-concentration cells. In their study, only about 5% of the influent flow passed through the PEM resulting in a poor nutrient recovery (i.e., the recovery of 1.2% of N and 0.002% of P). It is noteworthy that, if they were designed as an on-site system, their processes not only generate power and recover nutrients, but also save a large amount of water that is necessary to flush and transport urine to a central treatment facility.

4.2.5. MFC Natural Construction Material for Nutrient Recovery

Marzorati et al. [133] constructed an MFC using natural lingo-cellulosic materials and treated swine manure. In their MFC, an electro-osmotic flux created high pH conditions in the vicinity of the cathode, which induced deposition of nutrients such as N, K, Mg and Ca. The materials, especially maize stalks, underwent partial biodegradation, thus the elements of these materials could be released into the wastewater being treated [133]. Since infor-

mation about MFCs constructed using lingo-cellulosic materials is scarce, further research into these materials is needed to develop more effective MFCs for wastewater treatment.

4.2.6. Field Trial for Nutrient Recovery

The present work revealed that only a few studies have been conducted in the fields using pilot-scale or full-scale MFCs [16,88,174–178]. The past studies using pilot-scale MFCs have demonstrated that the MFCs can be self-sustainable [16,88,176]; that is, the energy captured by the MFCs was sufficient for powering the feed and recirculation pumps [127]. Ge & He [16] developed a 200-L modularized MFC system consisting of 96 MFC modules and treated primary effluent of a local WWTP. This study was one of the few field trials to treat actual wastewater for a long duration (>300 days). This system removed more than 75% of COD and 68% of NH_4^+ -N. On the other hand, the same MFC system did not perform well in removing P (~20%). In their system, P and N were accumulated, and thus, their MFC system required a further P and N disposal [16]. An accumulation of nitrate also occurred in the system due to nitrification. Despite the fact that the past studies have produced encouraging results, much work remains to be done in terms of treatment efficiency, energy efficiency, and cost-effectiveness [179,180]. Improvements in nutrient recovery must be made for the MFCs to be implemented as one of the renewable energy technologies.

Table 2. MFCs for nutrient removal/recovery from different types of wastewaters and operational conditions.

Type of Wastewater	System Type/Operation Mode	Initial Wastewater Characteristics	COD Removal/HRT	NH ₄ ⁺ -N Removal/Recovery	PO ₄ ³⁻ -P Removal/Recovery	Reference
Synthetic wastewater	Mediator-less dual chamber MFC 2-stage feed-batch mode (Two sets of dual-chamber H-type bottles, operated for 120 days)	COD: 1.5 g/L pH: >8	70–90% HRT = 48 h	—————	38% recovery	[103]
Primary effluent of municipal wastewater	200 L Modularized MFC system (96 tubular MFC modules of 2 L/each) Continuous mode, operated for one-year	TCOD: 155 ± 37 mg/L SCOD: 73 ± 23 mg/L NH ₄ ⁺ : 25.7 ± 5.5 mg/L TSS: 72.9 ± 16.6 mg/L pH: >8	>75% HRT = 18 h	68% removal	~20% biomass uptake	[16]
Dairy industrial wastewater	Catalyst-less and mediator-less membrane dual chamber MFC. Continuous mode.	COD: 3620 mg/L NH ₄ ⁺ : 174 mg/L Total P: 187 mg/L NH ₃ : 167 mg/L TSS: 1430 mg/L VSS: 647 mg/L BOD ₅ : 2115 mg/L pH: 8.5–10.3	90.46%	69.43% removal	Removal efficiencies: 31.18% dissolved phosphorus, 72.45% phosphorus in suspended solids	[48]
Untreated human urine	3-stage MFC system in a continuous mode (System of MFCs that fits urinals).	NH ₄ ⁺ : 363 mg/L PO ₄ ³⁻ : 202 mg/L	20% HRT = 18 min for individual MFCs for 5 days	20% removal 7% recovery	82% removal 78% recovery	[28]
Domestic wastewater	Algal biofilm MFC. Continuous mode.	COD: 186.8–327.9 mg/L Total N: 25.3–52.5 mg/L Total P: 2.9–8.3 mg/L	81.9% HRT = 12 days	TN removal: 95.5% 50% recovered by harvested algae	TP removal: 96.4% 62% recovered by harvested algae	[20]
Effluent drain of vegetable oil industry	Dual chambered MFC. Batch mode at 35 °C.	pH: 5.7 TDS: 517 mg/L TSS: 252 mg/L	60–90% 40–80% at 25 °C HRT = 72 h	—————	73.6% removal 56.9% at 25 °C	[147]
Digestate coming from an anaerobic digester	MET (MFC or MEC) coupled with struvite crystallization using seawater bitterns (SWB). Single chamber, air-cathode MFC batch mode.	NH ₄ ⁺ : 1943 ± 53 mg/L PO ₄ ³⁻ : 60 ± 3 mg/L COD: 7.2 ± 1.6 g/L	44.7 ± 1.6%	MFC: 10.1 ± 0.5% removal Further removal by precipitation: 14.7 ± 0.6%	MFC: 35.8 ± 1.2% removal Further removal by precipitation: 83.1 ± 3.7%	[151]
Pre-hydrolyzed human urine	Electrodialysis system embedded in an MFC. Continuous mode.	NH ₄ ⁺ : 7.8 g/L PO ₄ ³⁻ : 0.33 g/L TCOD: 9.5 g/L pH = 8.8	40–65 days	1.2% recovery	0.002% recovery	[15]
Synthetic domestic wastewater	Photoautotrophic H-type MFC. Continuous mode.	Inoculated microalgal biomass: 0.75 g/L	93.2% HRT = 11.8 h	95.9% removed in anodic chamber. 27.7–50.0% removed/recovery in cathodic chamber by microalgae.	82.7% removed in anodic chamber. 37.1–67.9% removed/recovery in cathodic chamber by microalgae.	[152]

Table 2. Cont.

Type of Wastewater	System Type/Operation Mode	Initial Wastewater Characteristics	COD Removal/HRT	NH ₄ ⁺ -N Removal/Recovery	PO ₄ ³⁻ -P Removal/Recovery	Reference
Synthetic domestic wastewater	Double-chamber MFC. Continuous mode.	COD: 300–600 mg/L OLR: 435–870 mg COD/L.d	90% (from a wide range of organic loading rate (435 to 870 mg COD/L.d). HRT = 0.69 d	Removed in anode chamber: 14% at OLR of 435 mg COD/L.d and 75.13% at OLR of 870 mg COD/L.d. Recovered in cathode chamber: 85.11% at OLR of 435 mg COD/L.d and 24.34% at OLR of 870 mg COD/L.d.	Removed in anode chamber: 12.43% at OLR of 435 mg COD/L.d and 71.5% at OLR of 870 mg COD/L.d. Recovered in cathode chamber: 24.4% average recovery.	[21]
Synthetic municipal wastewater	Double-compartment MFC. Continuous mode.	COD: 300 ± 15 mg/L NH ₄ ⁺ -N: 5–40 mg/L OLR: 435 mg COD/L.d	>85% for wide range of NH ₄ ⁺ -N concentrations (5 to 40 mg/L). HRT = 0.69 d	Removal: ~14% at 5 mg. NH ₄ ⁺ -N/L and ~14.10% at 40 mg. NH ₄ ⁺ -N/L. Recovery: 85.11% at 5 mg. NH ₄ ⁺ -N/L and 15.33% at 40 mg. NH ₄ ⁺ -N/L.	Removal: ~12.45% at 5 mg. NH ₄ ⁺ -N/L and 13.33% at 40 mg. NH ₄ ⁺ -N/L. Recovery: 83.23% at 5 mg. NH ₄ ⁺ -N/L and 80.5% at 40 mg. NH ₄ ⁺ -N/L.	[49]
Synthetic urine-containing wastewater	Three-chamber resource recovery MFC. Batch mode.	COD: 24.60 mg NH ₄ ⁺ : 0.10 mg TN: 20.20 mg PO ₄ ³⁻ : 0.90 mg pH: 6.9	97% HRT = ~3 days	40% of NH ₄ ⁺ removed. 98% of TN removed. 42% of TN recovered in middle chamber	99% removed. 37% recovered in middle chamber.	[17]
Synthetic municipal wastewater	Two-chambered MFC. Continuous mode.	COD: 300 ± 15 mg/L pH: 7.00 ± 0.02 OLR: 435–870 mg COD/L.d	>90% (from a wide range of organic loading rate (435 to 870 mg COD/L.d) and HRT = 0.69–0.35 days.	Removed in anode chamber: 13%–15% at different OLR (435–870 mg COD/L.d) and different HRT (0.69 d–0.35 d). Recovered in cathode chamber: ~85% at different OLR (435–870 mg COD/L.d) and different HRT (0.69 d–0.35 d).	Removed in anode chamber: 12–14% at different OLR (435–870 mg COD/L.d) and different HRT (0.69 d–0.35 d). Recovered in cathode chamber: ~83% at different OLR (435–870 mg COD/L.d) and different HRT (0.69 d–0.35 d).	[19]

5. Challenges and Directions for Optimization

MFC technologies can harvest clean energy from waste organic sources employing exoelectrogenic microorganisms [116,181,182]. Recently, MFC technologies have made considerable progress; however, these technologies are still facing great challenges concerning power generation, nutrient removal and/or recovery, and real-world applications. To become competitive with the present wastewater treatment technologies, future MFC research should focus on reducing electrochemical energy loss, increasing nutrient removal and/or recovery efficiencies, and improving effluent water quality.

Compared with conventional batteries, the power output of MFCs is low, which is the main barrier that is restricting commercialization and large-scale implementations of the MFC technologies [183–185]. To create more efficient MFCs, the Coulombic efficiency and voltage must be increased [128,186]. The performance of MFCs can be enhanced by developing or finding highly efficient, low resistance electrodes and separation membranes [119,187], and optimizing and controlling pH in the chambers [119,186].

The use of a suitable material for the anodes may improve biofilm formation and electron coupling. The anodes that have a large surface area and functional organic groups (e.g., carbon-based materials) can improve cell vitality. The conductive elements such as manganese and iron can be incorporated into the carbon-based electrodes to increase power output. To maximize the benefits of MFC technologies, further investigation should be conducted to understand the electron pathway mechanisms to minimize the electron transfer loss.

The problem with the electrode distancing can be resolved by changing the MFC design. For instance, Rossi & Logan [188] developed an H-cell MFC design in which they demonstrated that electrode distance was not important due to the difference in the cross-sectional area of the MFC and the projected areas of the electrodes. Another potential solution to electrode distancing may be the use of the simultaneous series-parallel connection of the electrodes. This design strategy can increase the voltage and current.

Developing or finding efficient, low resistance separation membranes is another hurdle to clear. The disadvantage of using PEM in the MFC design lies in the development of pH gradients between anode and cathode chambers, which causes energy loss [189]. Other hindrances associated with PEM are O₂ diffusion, H₂ loss, fluxes of carboxylates, and concentration overpotential across the membrane [190]. The fabrication of nanostructured anodes with a high surface area might offer an effective solution to reduce membrane resistance [191,192]. The membrane-less microfluidic systems can eliminate membrane resistance due to the laminar flow that keeps the anolyte and catholyte well separated [193–196].

Electrolyte pH is crucial to the MFC power output and nutrient removal and/or recovery. Although the traditional dual-chamber MFCs can maintain two different pH conditions to optimize the anodic and cathodic reactions, such conditions are unattainable in the single-chamber MFCs [121]. In this respect, the multiple-chamber MFCs offer advantages over the single-chamber MFCs by enhancing the removal and/or recovery of P and N [19,21,49,147]. On the other hand, single-chamber MFCs assembled in series can produce higher power output than dual-chamber MFCs [197].

The MFC technologies have immense application potential especially in the regions where electrical infrastructure and water sanitation are lacking [121,198]. More studies should focus on field demonstrations using real wastewaters aiming at practical applications.

6. Conclusions

Microbial fuel cells (MFCs) are bioelectrochemical devices that use microorganisms to degrade organic pollutants while simultaneously generating electricity. This review paper presented and discussed published studies on the different types of MFCs that have been used for resource recovery from various wastewaters. This review especially focused on the removal and recovery of phosphorus (P), nitrogen (N), and organics (COD).

MFCs could serve as a feasible technology to remove and/or recover nutrients from a wide range of wastewaters, in addition, to remove organic pollutants and simultaneously generating electricity. Removal of P and N in an MFC can be accomplished by assimilation, and N can also be removed by volatilization. The recovery of P and N can be accomplished in the form of struvite, which can be utilized as a slow-release fertilizer. The multiple-chamber MFC offers the advantage over the single-chamber MFCs in terms of enhancing the removal and/or recovery of P and N. Because the precipitation of struvite on the cathode surface reduces the MFC efficiency, the MFCs may be designed to have removable cathode electrodes that can be cleaned instead of replacing them when their efficiency falls [50].

Continuous operation of the MFC system requires an energy input such as energy for pumping a feed solution to the MFC. Some of the previous works have shown that the WWTP operation cost can be offset by recovering nutrient and bioenergy from domestic and industrial wastewater. Although researchers have demonstrated that nutrients could be removed or recovered and concurrently generating electricity, most studies have been conducted on a laboratory scale, and very few studies have used a full-scale wastewater treatment facility. Furthermore, the power generation remains low. Therefore, innovation is required for developing more efficient MFC technology that is applicable to large-scale facilities.

Author Contributions: Conceptualization, data collection, and writing—original draft preparation, N.E.P.; critical revision and edition, C.S. Both authors have read and agreed to the published version of the manuscript.

Funding: This research received no external funding.

Institutional Review Board Statement: Not applicable.

Informed Consent Statement: Not applicable.

Data Availability Statement: Not applicable.

Conflicts of Interest: The authors declare no conflict of interest.

References

1. Reddy, C.D.; Nguyen, H.T.; Noori, M.T.; Min, B. Potential applications of algae in the cathode of microbial fuel cells for enhanced electricity generation with simultaneous nutrient removal and algae biorefinery: Current statuses and future perspectives. *Bioresour. Technol.* **2019**, *292*, 122010. [CrossRef] [PubMed]
2. Jingyu, H.; Miwornunyuie, N.; Ewusi-Mensah, D.; Koomson, D.A. Assessing the factors influencing the performance of constructed wetland-microbial fuel cell integration. *Water Sci. Technol.* **2020**, *81*, 631–643. [CrossRef] [PubMed]
3. UN Environment Annual Report 2017. Available online: <https://www.unenvironment.org/annualreport/2017/index.php> (accessed on 20 March 2020).
4. Tilman, D.; Balzer, C.; Hill, J.; Befort, B.L. Global food demand and the sustainable intensification of agriculture. *Proc. Natl. Acad. Sci. USA* **2011**, *108*, 20260–20264. [CrossRef]
5. Chen, X.; Sun, D.; Zhang, X.; Liang, P.; Huang, X. Novel self-driven microbial nutrient recovery cell with simultaneous wastewater purification. *Sci. Rep.* **2015**, *5*, 15744. [CrossRef] [PubMed]
6. Gardner-Dale, D.A.; Bradley, I.M.; Guest, J.S. Influence of solids residence time and carbon storage on nitrogen and phosphorus recovery by microalgae across diel cycles. *Water Res.* **2017**, *121*, 231–239. [CrossRef] [PubMed]
7. Electric Power Research Institute (EPRI). *Water & Sustainability: U.S. Electricity Consumption for the Water Supply & Treatment. The Next Half Century Topical Report*; EPRI: Palo Alto, CA, USA, 2002.
8. U.S. Department of Energy. *The Water-Energy Nexus: Challenges and Opportunities*; U.S. Department of Energy: Washington, DC, USA, 2014.
9. Callegari, A.; Cecconet, D.; Molognoni, D.; Capodaglio, A.G. Sustainable processing of dairy wastewater: Long-term pilot application of a bio-electrochemical system. *J. Clean. Prod.* **2018**, *189*, 563–569. [CrossRef]
10. Gu, Y.; Li, Y.; Li, X.; Luo, P.; Wang, H.; Robinson, Z.P.; Wang, X.; Wu, J.; Li, F. The feasibility and challenges of energy self-sufficient wastewater treatment plants. *Appl. Energy* **2017**, *204*, 1463–1475. [CrossRef]
11. Li, W.; Li, L.; Qiu, G. Energy consumption and economic cost of typical wastewater treatment systems in Shenzhen, China. *J. Clean. Prod.* **2017**, *163*, S374–S378. [CrossRef]
12. Xu, J.; Luo, P.; Lu, B.; Wang, H.; Wang, X.; Wu, J.; Yan, J. Energy-water nexus analysis of wastewater treatment plants (WWTPs) in China based on statistical methodologies. *Energy Procedia* **2018**, *152*, 259–264. [CrossRef]

13. Yu, Y.; Zou, Z.; Wang, S. Statistical regression modeling for energy consumption in wastewater treatment. *J. Environ. Sci.* **2019**, *75*, 201–208. [[CrossRef](#)]
14. Shannon, M.A.; Bohn, P.W.; Elimelech, M.; Georgiadis, J.G.; Mariñas, B.J.; Mayes, A.M. Science and technology for water purification in the coming decades. *Nat. Cell Biol.* **2008**, *452*, 301–310. [[CrossRef](#)]
15. Freguia, S.; Logrieco, M.E.; Monetti, J.; Ledezma, P.; Viridis, B.; Tsujimura, S. Self-powered bioelectrochemical nutrient recovery for fertilizer generation from human urine. *Sustainability* **2019**, *11*, 5490. [[CrossRef](#)]
16. Ge, Z.; He, Z. Long-term performance of a 200 liter modularized microbial fuel cell system treating municipal wastewater: Treatment, energy, and cost. *Environ. Sci. Water Res. Technol.* **2016**, *2*, 274–281. [[CrossRef](#)]
17. Lu, S.; Li, H.; Tan, G.; Wen, F.; Flynn, M.T.; Zhu, X. Resource recovery microbial fuel cells for urine-containing wastewater treatment without external energy consumption. *Chem. Eng. J.* **2019**, *373*, 1072–1080. [[CrossRef](#)]
18. Yan, T.; Ye, Y.; Ma, H.; Zhang, Y.; Guo, W.; Du, B.; Wei, Q.; Wei, D.; Ngo, H.H. A critical review on membrane hybrid system for nutrient recovery from wastewater. *Chem. Eng. J.* **2018**, *348*, 143–156. [[CrossRef](#)]
19. Ye, Y.; Ngo, H.H.; Guo, W.; Chang, S.W.; Nguyen, D.D.; Zhang, X.; Zhang, S.; Luo, G.; Liu, Y. Impacts of hydraulic retention time on a continuous flow mode dual-chamber microbial fuel cell for recovering nutrients from municipal wastewater. *Sci. Total Environ.* **2020**, *734*, 139220. [[CrossRef](#)]
20. Yang, Z.; Pei, H.; Hou, Q.; Jiang, L.; Zhang, L.; Nie, C. Algal biofilm-assisted microbial fuel cell to enhance domestic wastewater treatment: Nutrient, organics removal and bioenergy production. *Chem. Eng. J.* **2018**, *332*, 277–285. [[CrossRef](#)]
21. Ye, Y.; Ngo, H.H.; Guo, W.; Chang, S.W.; Nguyen, D.D.; Liu, Y.; Nghiem, L.; Zhang, X.; Wang, J. Effect of organic loading rate on the recovery of nutrients and energy in a dual-chamber microbial fuel cell. *Bioresour. Technol.* **2019**, *281*, 367–373. [[CrossRef](#)]
22. Brito, P.S.D.; Sequeira, C.A.C. Electrochemical generators and the environment. Fuel cells and metal/air batteries. *Stud. Environ. Sci.* **1994**, *59*, 203–221.
23. Paucar, N.E.; Kiggins, P.; Blad, B.; De Jesus, K.; Afrin, F.; Pashikanti, S.; Sharma, K. Ionic liquids for the removal of sulfur and nitrogen compounds in fuels: A review. *Environ. Chem. Lett.* **2020**, *19*, 1205–1228. [[CrossRef](#)]
24. Yao, L.; Yang, B.; Cui, H.; Zhuang, J.; Ye, J.; Xue, J. Challenges and progresses of energy storage technology and its application in power systems. *J. Mod. Power Syst. Clean Energy* **2016**, *4*, 519–528. [[CrossRef](#)]
25. Matsuda, Y.; Shimizu, T.; Hashimasa, Y. Effect of carbon monoxide on polymer electrolyte fuel cell performance with a hydrogen circulation system. *J. Electrochem. Soc.* **2020**, *167*, 044509. [[CrossRef](#)]
26. Zhang, H.; Sun, C. Cost-effective iron-based aqueous redox flow batteries for large-scale energy storage application: A review. *J. Power Sources* **2021**, *493*, 229445. [[CrossRef](#)]
27. Appleby, A.J.; Foulkes, F.R. *Fuel Cell Handbook*, 1st ed.; Van Nostrand Reinhold: New York, NY, USA, 1989; p. 261.
28. You, J.; Greenman, J.; Melhuish, C.; Ieropoulos, I. Electricity generation and struvite recovery from human urine using microbial fuel cells. *J. Chem. Technol. Biotechnol.* **2016**, *91*, 647–654. [[CrossRef](#)]
29. Zhou, Y.; Wang, L.; Zhou, Y.; Mao, X.Z. Eutrophication control strategies for highly anthropogenic influenced coastal waters. *Sci. Total Environ.* **2020**, *705*, 135760. [[CrossRef](#)] [[PubMed](#)]
30. Chen, X.; Zhou, H.; Zuo, K.; Zhou, Y.; Wang, Q.; Sun, D.; Gao, Y.; Liang, P.; Zhang, X.; Ren, Z.J.; et al. Self-sustaining advanced wastewater purification and simultaneous in situ nutrient recovery in a novel bioelectrochemical system. *Chem. Eng. J.* **2017**, *330*, 692–697. [[CrossRef](#)]
31. Cordell, D.; Rosemarin, A.; Schröder, J.J.; Smit, A.L. Towards global phosphorus security: A systems framework for phosphorus recovery and reuse options. *Chemosphere* **2011**, *84*, 747–758. [[CrossRef](#)] [[PubMed](#)]
32. Smil, V. Phosphorus in the environment: Natural flows and human interference. *Annu. Rev. Energy Environ.* **2000**, *25*, 53–88. [[CrossRef](#)]
33. Cordell, D.; White, S. Peak phosphorus: Clarifying the key issues of a vigorous debate about long-term phosphorus security. *Sustainability* **2011**, *3*, 2027–2049. [[CrossRef](#)]
34. Rittmann, B.E.; Mayer, B.; Westerhoff, P.; Edwards, M. Capturing the lost phosphorus. *Chemosphere* **2011**, *84*, 846–853. [[CrossRef](#)] [[PubMed](#)]
35. Geerts, S.; Marchi, A.; Weemaes, M. Full-scale phosphorus recovery from digested wastewater sludge in Belgium-part II: Economic opportunities and risks. *Water Sci. Technol.* **2015**, *71*, 495–502. [[CrossRef](#)]
36. Marchi, A.; Geerts, S.; Weemaes, M.; Wim, S.; Christine, V. Full-scale phosphorus recovery from digested waste water sludge in Belgium-part I: Technical achievements and challenges. *Water Sci. Technol.* **2015**, *71*, 487–494. [[CrossRef](#)]
37. Mihelcic, J.R.; Fry, L.M.; Shaw, R. Global potential of phosphorus recovery from human urine and feces. *Chemosphere* **2011**, *84*, 832–839. [[CrossRef](#)]
38. Erisman, J.W.; Sutton, M.A.; Galloway, J.; Klimont, Z.; Winiwarter, W. How a century of ammonia synthesis changed the world. *Nat. Geosci.* **2008**, *1*, 636–639. [[CrossRef](#)]
39. Fowler, D.; Coyle, M.; Skiba, U.; Sutton, M.A.; Cape, N.; Reis, S.; Sheppard, L.J.; Jenkins, A.; Grizzatti, B.; Galloway, J.N.; et al. The global nitrogen cycle in the twenty-first century. *Philos. Trans. R. Soc. B* **2013**, *368*, 20130164. [[CrossRef](#)] [[PubMed](#)]
40. He, C.; Chen, Y.; Liu, C.; Jiang, Y.; Yin, R.; Qiu, T. The role of reagent adding sequence in the NH₄⁺-N recovery by MAP method. *Sci. Rep.* **2020**, *10*, 7672. [[CrossRef](#)] [[PubMed](#)]
41. Nancharaiyah, Y.V.; Reddy, G.K.K. Aerobic granular sludge technology: Mechanisms of granulation and biotechnological applications. *Bioresour. Technol.* **2017**, *247*, 1128–1143. [[CrossRef](#)]

42. Kuntke, P.; Śmiech, K.M.; Bruning, H.; Zeeman, G.; Saakes, M.; Sleutels, T.H.J.A.; Hamelers, H.V.M.; Buisman, C.J.N. Ammonium recovery and energy production from urine by a microbial fuel cell. *Water Res.* **2012**, *46*, 2627–2636. [[CrossRef](#)]
43. Maurer, M.; Pronk, W.; Larsen, T.A. Treatment processes for source-separated urine. *Water Res.* **2006**, *40*, 3151–3166. [[CrossRef](#)] [[PubMed](#)]
44. Iskander, S.M.; Brazil, B.; Novak, J.T.; He, Z. Resource recovery from landfill leachate using bioelectrochemical systems: Opportunities, challenges, and perspectives. *Bioresour. Technol.* **2016**, *201*, 347–354. [[CrossRef](#)]
45. Bodirsky, B.L.; Popp, A.; Lotze-Campen, H.; Dietrich, J.P.; Rolinski, S.; Weindl, I.; Schmitz, C.; Müller, C.; Bonsch, M.; Humpenöder, F.; et al. Reactive nitrogen requirements to feed the world in 2050 and potential to mitigate nitrogen pollution. *Nat. Commun.* **2014**, *5*, 3858. [[CrossRef](#)]
46. Foley, J.; De Haas, D.; Hartley, K.; Lant, P. Comprehensive life cycle inventories of alternative wastewater treatment systems. *Water Res.* **2010**, *44*, 1654–1666. [[CrossRef](#)]
47. Ledezma, P.; Kuntke, P.; Buisman, C.J.; Keller, J.; Freguia, S. Source-separated urine opens golden opportunities for microbial electrochemical technologies. *Trends Biotechnol.* **2015**, *33*, 214–220. [[CrossRef](#)]
48. Mansoorian, H.J.; Mahvi, A.H.; Jafari, A.J.; Khanjani, N. Evaluation of dairy industry wastewater treatment and simultaneous bioelectricity generation in a catalyst-less and mediator-less membrane microbial fuel cell. *J. Saudi Chem. Soc.* **2016**, *20*, 88–100. [[CrossRef](#)]
49. Ye, Y.; Ngo, H.H.; Guo, W.; Chang, S.W.; Nguyen, D.D.; Liu, Y.; Ni, B.-J.; Zhang, X. Microbial fuel cell for nutrient recovery and electricity generation from municipal wastewater under different ammonium concentrations. *Bioresour. Technol.* **2019**, *292*, 121992. [[CrossRef](#)]
50. Kelly, P.T.; He, Z. Nutrients removal and recovery in bioelectrochemical systems: A review. *Bioresour. Technol.* **2014**, *153*, 351–360. [[CrossRef](#)]
51. Tao, W.; Fattah, K.P.; Huchzermeier, M.P. Struvite recovery from anaerobically digested manure: A review. *J. Environ. Manag.* **2016**, *169*, 46–57. [[CrossRef](#)]
52. Hermassi, M.; Valderrama, C.; Gibert, O.; Moreno, N.; Querol, X.; Batis, N.H.; Cortina, J.L. Recovery of nutrients (N-P-K) from potassium-rich sludge anaerobic digestion side-streams by integration of a hybrid sorption-membrane ultrafiltration process: Use of powder reactive sorbents as nutrient carriers. *Sci. Total Environ.* **2017**, *599*, 422–430. [[CrossRef](#)] [[PubMed](#)]
53. Logan, B.E.; Hamelers, B.; Rozendal, R.; Schröder, U.; Keller, J.; Freguia, S.; Aelterman, P.; Verstraete, W.; Rabaey, K. Microbial fuel cells: Methodology and technology. *Environ. Sci. Technol.* **2006**, *40*, 5181–5192. [[CrossRef](#)] [[PubMed](#)]
54. Rahimnejad, M.; Ghoreyshi, A.; Najafpour, G.; Younesi, H.; Shakeri, M. A novel microbial fuel cell stack for continuous production of clean energy. *Int. J. Hydrogen Energy* **2012**, *37*, 5992–6000. [[CrossRef](#)]
55. Oon, Y.L.; Ong, S.A.; Ho, L.N.; Wong, Y.S.; Oon, Y.S.; Lehl, H.K.; Thung, W.E. Hybrid system up-flow constructed wetland integrated with microbial fuel cell for simultaneous wastewater treatment and electricity generation. *Bioresour. Technol.* **2015**, *186*, 270–275. [[CrossRef](#)] [[PubMed](#)]
56. Rossi, R.; Jones, D.; Myung, J.; Zikmund, E.; Yang, W.; Gallego, Y.A.; Pant, D.; Evans, P.J.; Page, M.A.; Crokek, D.M.; et al. Evaluating a multi-panel air cathode through electrochemical and biotic tests. *Water Res.* **2019**, *148*, 51–59. [[CrossRef](#)]
57. Gude, V.G. Wastewater treatment in microbial fuel cells—An overview. *J. Clean. Prod.* **2016**, *122*, 287–307. [[CrossRef](#)]
58. Zhuang, L.; Zhou, S.; Wang, Y.; Liu, C.; Geng, S. Membrane-less cloth cathode assembly (CCA) for scalable microbial fuel cells. *Biosens. Bioelectron.* **2009**, *24*, 3652–3656. [[CrossRef](#)] [[PubMed](#)]
59. Zuo, Y.; Cheng, S.; Call, D.; Logan, B.E. Tubular Membrane Cathodes for Scalable Power Generation in Microbial Fuel Cells. *Environ. Sci. Technol.* **2007**, *41*, 3347–3353. [[CrossRef](#)]
60. Hernández-Fernández, F.J.; de los Ríos, A.P.; Mateo-Ramírez, F.; Godínez, C.; Lozano-Blanco, L.J.; Moreno, J.I.; Tomás-Alonso, F. New application of supported ionic liquids membranes as proton exchange membranes in microbial fuel cell for waste water treatment. *Chem. Eng. J.* **2015**, *279*, 115–119. [[CrossRef](#)]
61. Beizhen, X.; Bojie, L.; Shaoquiang, Y.; Hong, L. Denitrification and electrogenesis performances of bio-cathode microbial fuel cells with carbon paper separator. *Chin. J. Environ. Eng.* **2014**, *8*, 2163–2168.
62. Bond, D.R.; Lovley, D.R. Electricity production by *Geobacter sulfurreducens* attached to electrodes. *Appl. Environ. Microbiol.* **2003**, *69*, 1548–1555. [[CrossRef](#)]
63. Rabaey, K.; Lissens, G.; Siciliano, S.D.; Verstraete, W. A microbial fuel cell capable of converting glucose to electricity at high rate and efficiency. *Biotechnol. Lett.* **2003**, *25*, 1531–1535. [[CrossRef](#)] [[PubMed](#)]
64. Chaijak, P.; Sato, C.; Lertworapreecha, M.; Sukkasem, C.; Boonsawang, P.; Paucar, N.E. Potential of biochar-anode in a ceramic-separator microbial fuel cell (CMFC) with a laccase-based air cathode. *Pol. J. Environ. Stud.* **2019**, *29*, 499–503. [[CrossRef](#)]
65. Tremouli, A.; Greenman, J.; Ieropoulos, I. Investigation of ceramic MFC stacks for urine energy extraction. *Bioelectrochemistry* **2018**, *123*, 19–25. [[CrossRef](#)]
66. Winfield, J.; Gajda, I.; Greenman, J.; Leroulos, I. A review into the use of ceramics in microbial fuel cells. *Bioresour. Technol.* **2016**, *215*, 296–303. [[CrossRef](#)]
67. Das, S.; Mangwani, N. Recent developments in microbial fuel cells: A review. *J. Sci. Ind. Res.* **2010**, *69*, 727–731.
68. Madigan, M.T.; Martinko, J.M.; Parker, J. *Brock Biology of Microorganisms*, 9th ed.; Prentice Hall: Upper Saddle River, NJ, USA, 2000.
69. Sharma, Y.; Li, B. Optimizing energy harvest in wastewater treatment by combining anaerobic hydrogen producing biofermentor (HPB) and microbial fuel cell (MFC). *Int. J. Hydrogen Energy* **2010**, *35*, 3789–3797. [[CrossRef](#)]

70. Nimje, V.R.; Chen, C.Y.; Chen, H.R.; Chen, C.C.; Huang, Y.M.; Tseng, M.J.; Cheng, K.C.; Chang, Y.F. Comparative bioelectricity production from various wastewaters in microbial fuel cells using mixed cultures and a pure strain of *Shewanella oneidensis*. *Bioresour. Technol.* **2012**, *104*, 315–323. [[CrossRef](#)] [[PubMed](#)]
71. Zhi, W.; Ge, Z.; He, Z.; Zhang, H. Methods for understanding microbial community structures and functions in microbial fuel cells: A review. *Bioresour. Technol.* **2014**, *171*, 461–468. [[CrossRef](#)] [[PubMed](#)]
72. Walter, X.A.; Greenman, J.; Ieropoulos, I.A. Microbial fuel cells directly powering a microcomputer. *J. Power Sources* **2020**, *446*, 227328. [[CrossRef](#)] [[PubMed](#)]
73. Corbella, C.; Garfi, M.; Puigagut, J. Vertical redox profiles in treatment wetlands as function of hydraulic regime and macrophytes presence: Surveying the optimal scenario for microbial fuel cell implementation. *Sci. Total Environ.* **2014**, *470*, 754–758. [[CrossRef](#)]
74. Li, Z.; Haynes, R.; Sato, E.; Shields, M.S.; Fujita, Y.; Sato, C. Microbial community analysis of a single chamber microbial fuel cell using potato wastewater. *Water Environ. Res.* **2014**, *86*, 324–330. [[CrossRef](#)]
75. Logan, B.E. Exoelectrogenic bacteria that power microbial fuel cells. *Nat. Rev. Microbiol.* **2009**, *7*, 375–381. [[CrossRef](#)]
76. Bonanni, P.S.; Schrott, G.D.; Robuschi, L.; Busalmen, J.P. Charge accumulation and electron transfer kinetics in *Geobacter sulfurreducens* biofilms. *Energy Environ. Sci.* **2012**, *5*, 6188–6195. [[CrossRef](#)]
77. Busalmen, J.P.; Esteve-Nuñez, A.; Feliu, J.M. Whole cell electrochemistry of electricity-producing microorganisms evidence an adaptation for optimal exocellular electron transport. *Environ. Sci. Technol.* **2008**, *42*, 2445–2450. [[CrossRef](#)] [[PubMed](#)]
78. Arends, J.B.; Verstraete, W. 100 years of microbial electricity production: Three concepts for the future. *Microb. Biotechnol.* **2012**, *5*, 333–346. [[CrossRef](#)]
79. Ramírez-Vargas, C.A.; Arias, C.A.; Zhang, L.; Brix, H. Microbial community function in electroactive biofilm-based constructed wetlands. *Biogeosci. Discuss.* **2018**, 1–28. [[CrossRef](#)]
80. Delaney, G.M.; Bennetto, H.P.; Mason, J.R.; Roller, S.D.; Stirling, J.L.; Thurston, C.F. Electron-transfer coupling in microbial fuel cells. 2. Performance of fuel cells containing selected microorganism-mediator-substrate combinations. *J. Chem. Technol. Biotechnol.* **1984**, *34*, 13–27. [[CrossRef](#)]
81. Bosire, E.M.; Blank, L.M.; Rosenbaum, M.A. Strain-and substrate-dependent redox mediator and electricity production by *Pseudomonas aeruginosa*. *Appl. Environ. Microbiol.* **2016**, *82*, 5026–5038. [[CrossRef](#)]
82. Lovley, D.R. The microbe electric: Conversion of organic matter to electricity. *Curr. Opin. Biotechnol.* **2008**, *19*, 564–571. [[CrossRef](#)] [[PubMed](#)]
83. Palmore, G.T.R.; Kim, H.H. Electro-enzymatic reduction of dioxygen to water in the cathode compartment of a biofuel cell. *J. Electroanal. Chem.* **1999**, *464*, 110–117. [[CrossRef](#)]
84. Heijne, A.T.; Liu, F.; Weijden, R.V.D.; Weijma, J.; Buisman, C.J.; Hamelers, H.V. Copper recovery combined with electricity production in a microbial fuel cell. *Environ. Sci. Technol.* **2010**, *44*, 4376–4381. [[CrossRef](#)]
85. Pant, D.; van Bogaert, G.; Diels, L. A review of the substrates used in microbial fuel cells (MFCs) for sustainable energy production. *Bioresour. Technol.* **2010**, *101*, 1533–1543. [[CrossRef](#)]
86. Pandey, P.; Shinde, V.N.; Deopurkar, R.L.; Kale, S.P.; Patil, S.A.; Pant, D. Recent advances in the use of different substrates in microbial fuel cells toward wastewater treatment and simultaneous energy recovery. *Appl. Energy* **2016**, *168*, 706–723. [[CrossRef](#)]
87. Akiba, T.; Bennetto, H.P.; Stirling, J.L.; Tanaka, K. Electricity production from alkalophilic organisms. *Biotechnol. Lett.* **1987**, *9*, 611–616. [[CrossRef](#)]
88. Dong, Y.; Qu, Y.; He, W.; Du, Y.; Liu, J.; Han, X.; Feng, Y. A 90-liter stackable baffled microbial fuel cell for brewery wastewater treatment based on energy self-sufficient mode. *Bioresour. Technol.* **2015**, *195*, 66–72. [[CrossRef](#)]
89. Gil, G.C.; Chang, I.S.; Kim, B.H.; Kim, M.; Jang, J.K.; Park, H.S.; Kim, H.J. Operational parameters affecting the performance of a mediator-less microbial fuel cell. *Biosens. Bioelectron.* **2003**, *18*, 327–334. [[CrossRef](#)]
90. He, L.; Du, P.; Chen, Y.; Lu, H.; Cheng, X.; Chang, B.; Wang, Z. Advances in microbial fuel cells for wastewater treatment. *Renew. Sustain. Energy Rev.* **2017**, *71*, 388–403. [[CrossRef](#)]
91. Li, W.W.; Yu, H.Q.; He, Z. Towards sustainable wastewater treatment by using microbial fuel cells-centered technologies. *Energy Environ. Sci.* **2014**, *7*, 911–924. [[CrossRef](#)]
92. Lu, M.; Chen, S.; Babanova, S.; Phadke, S.; Salvacion, M.; Mirhosseini, A.; Chan, S.; Carpenter, K.; Cortese, R.; Bretschger, O. Long-term performance of a 20-L continuous flow microbial fuel cell for treatment of brewery wastewater. *J. Power Sources* **2017**, *356*, 274–287. [[CrossRef](#)]
93. Seo, Y.; Kang, H.; Chang, S.; Lee, Y.-Y.; Cho, K.-S. Effects of nitrate and sulfate on the performance and bacterial community structure of membrane-less single-chamber air-cathode microbial fuel cells. *J. Environ. Sci. Health Part A* **2017**, *53*, 13–24. [[CrossRef](#)] [[PubMed](#)]
94. Zhang, Y.; Liu, M.; Zhou, M.; Yang, H.; Liang, L.; Gu, T. Microbial fuel cell hybrid systems for wastewater treatment and bioenergy production: Synergistic effects, mechanisms and challenges. *Renew. Sustain. Energy Rev.* **2019**, *103*, 13–29. [[CrossRef](#)]
95. Kim, B.H.; Chang, I.S.; Gadd, G.M. Challenges in microbial fuel cell development and operation. *Appl. Microbiol. Biotechnol.* **2007**, *76*, 485–494. [[CrossRef](#)]
96. Lefebvre, O.; Shen, Y.; Tan, Z.; Uzabiaga, A.; Chang, I.S.; Ng, H.Y. A comparison of membranes and enrichment strategies for microbial fuel cells. *Bioresour. Technol.* **2011**, *102*, 6291–6294. [[CrossRef](#)] [[PubMed](#)]
97. Rabaey, K.; Verstraete, W. Microbial fuel cells: Novel biotechnology for energy generation. *Trends Biotechnol.* **2005**, *23*, 291–298. [[CrossRef](#)] [[PubMed](#)]

98. Zhang, F.; Ge, Z.; Grimaud, J.; Hurst, J.; He, Z. Long-Term Performance of Liter-Scale Microbial Fuel Cells Treating Primary Effluent Installed in a Municipal Wastewater Treatment Facility. *Environ. Sci. Technol.* **2013**, *47*, 4941–4948. [[CrossRef](#)]
99. Do, M.H.; Ngo, H.H.; Guo, W.S.; Liu, Y.; Chang, S.W.; Nguyen, D.D.; Nghiem, L.D.; Ni, B.J. Challenges in the application of microbial fuel cells to wastewater treatment and energy production: A mini review. *Sci. Total Environ.* **2018**, *639*, 910–920. [[CrossRef](#)]
100. Jadhav, G.S.; Ghangrekar, M.M. performance of microbial fuel cell subjected to variation in pH, temperature, external load and substrate concentration. *Bioresour. Technol.* **2009**, *100*, 717–723. [[CrossRef](#)]
101. Jatoi, A.S.; Akhter, F.; Mazari, A.A.; Sabzoi, N.; Aziz, S.; Soomro, A.A.; Mubarak, N.M.; Baloch, H.; Memon, A.Q.; Ahmed, S. Advanced microbial fuel cell for waste water treatment—A review. *Environ. Sci. Pollut. Res.* **2020**, *28*, 5005–5019. [[CrossRef](#)] [[PubMed](#)]
102. Patroescu, V.; Jinescu, C.; Cosma, C.; Cristea, I.; Badescu, V.; Stefan, C.S. Influence of ammonium ion on the treatment process selection of groundwater supplies intended to human consumption. *Rev. Chim.* **2015**, *66*, 537–541.
103. Almatouq, A.; Babatunde, A.O. Concurrent phosphorus recovery and energy generation in mediator-less dual chamber microbial fuel cells: Mechanisms and influencing factors. *Int. J. Environ. Res. Public Health* **2016**, *13*, 375. [[CrossRef](#)] [[PubMed](#)]
104. Logan, B.E.; Regan, J.M. Microbial fuel cell: Challenges and technology. *Environ. Sci. Technol.* **2006**, *40*, 5172–5180. [[CrossRef](#)]
105. Xu, L.; Zhao, Y.; Doherty, L.; Hu, Y.; Hao, X. The integrated processes for wastewater treatment based on the principle of microbial fuel cells: A review. *Crit. Rev. Environ. Sci. Technol.* **2016**, *46*, 60–91. [[CrossRef](#)]
106. Lu, N.; Zhou, S.; Zhuang, L.; Zhang, J.; Ni, J. Electricity generation from starch processing wastewater using microbial fuel cell technology. *Biochem. Eng. J.* **2009**, *43*, 246–251. [[CrossRef](#)]
107. Puig, S.; Coma, M.; Desloover, J.; Boon, N.; Colprim, J.S.; Balaguer, M.D. Autotrophic denitrification in microbial fuel cells treating low ionic strength waters. *Environ. Sci. Technol.* **2012**, *46*, 2309–2315. [[CrossRef](#)]
108. Mardanpour, M.M.; Yaghmaei, S.; Kalantar, M. Modeling of microfluidic microbial fuel cells using quantitative bacterial transport parameters. *J. Power Sources* **2017**, *342*, 1017–1031. [[CrossRef](#)]
109. Corbella, C.; Puigagut, J. Improving domestic wastewater treatment efficiency with constructed wetland microbial fuel cells: Influence of anode material and external resistance. *Sci. Total Environ.* **2018**, *631*, 1406–1414. [[CrossRef](#)]
110. Ramírez-Vargas, C.A.; Prado, A.; Arias, C.A.; Carvalho, P.N.; Esteve-Núñez, A.; Brix, H. Microbial Electrochemical Technologies for Wastewater Treatment: Principles and Evolution from Microbial Fuel Cells to Bioelectrochemical-Based Constructed Wetlands. *Water* **2018**, *10*, 1128. [[CrossRef](#)]
111. Tamta, P.; Rani, N.; Yadav, A.K. Enhanced wastewater treatment and electricity generation using stacked constructed wetland-microbial fuel cells. *Environ. Chem. Lett.* **2020**, *18*, 871–879. [[CrossRef](#)]
112. Di Lorenzo, M.; Scott, K.; Curtis, T.P.; Head, I.M. Effect of increasing anode surface area on the performance of a single chamber microbial fuel cell. *Chem. Eng. J.* **2010**, *156*, 40–48. [[CrossRef](#)]
113. Hiegemann, H.; Herzer, D.; Nettmann, E.; Lübken, M.; Schulte, P.; Schmelz, K.G.; Gredigk-Hoffmann, S.; Wichern, M. An integrated 45 L pilot microbial fuel cell system at a full-scale wastewater treatment plant. *Bioresour. Technol.* **2016**, *218*, 115–122. [[CrossRef](#)]
114. Chiranjeevi, P.; Patil, S.A. Strategies for improving the electroactivity and specific metabolic functionality of microorganisms for various microbial electrochemical technologies. *Biotechnol. Adv.* **2020**, *39*, 107468. [[CrossRef](#)]
115. Gadkari, S.; Gu, S.; Sadhukhan, J. Towards automated design of bioelectrochemical systems: A comprehensive review of mathematical models. *Chem. Eng. J.* **2018**, *343*, 303–316. [[CrossRef](#)]
116. Gadkari, S.; Fontmorin, J.M.; Yu, E.; Sadhukhan, J. Influence of temperature and other system parameters on microbial fuel cell performance: Numerical and experimental investigation. *Chem. Eng. J.* **2020**, *388*, 12176. [[CrossRef](#)]
117. Fan, L.; Shi, J.; Xi, Y. PDVF-modified Nafion membrane for improved performance of MFC. *Membranes* **2020**, *10*, 185. [[CrossRef](#)] [[PubMed](#)]
118. Modestra, J.A.; Reddy, C.N.; Krishna, K.V.; Min, B.; Mohan, S.V. Regulated surface potential impacts bioelectrogenic activity, interfacial electron transfer and microbial dynamics in microbial fuel cell. *Renew. Energy* **2020**, *149*, 424–434. [[CrossRef](#)]
119. Fan, Y.; Sharbrough, E.; Liu, H. Quantification of the internal resistance distribution of microbial fuel cells. *Environ. Sci. Technol.* **2008**, *42*, 8101–8107. [[CrossRef](#)] [[PubMed](#)]
120. Liang, P.; Huang, X.; Fan, M.Z.; Cao, X.X.; Wang, C. Composition and distribution of internal resistance in three types of microbial fuel cells. *Appl. Microbiol. Biotechnol.* **2007**, *77*, 551–558. [[CrossRef](#)]
121. ElMekawy, A.; Hegab, H.M.; Dominguez-Benetton, X.; Pant, D. Internal resistance of microfluidic microbial fuel cell: Challenges and potential opportunities. *Bioresour. Technol.* **2013**, *142*, 672–682. [[CrossRef](#)] [[PubMed](#)]
122. He, Z.; Wagner, N.; Minteer, S.D.; Angenent, L.T. An upflow microbial fuel cell with an interior cathode: Assessment of the internal resistance by impedance spectroscopy. *Environ. Sci. Technol.* **2006**, *40*, 5212–5217. [[CrossRef](#)]
123. Khan, M.J.; Iqbal, M.T. Modelling and analysis of electrochemical, thermal, and reactant flow dynamics for a PEM fuel cell system. *Fuel Cells* **2005**, *4*, 463–475. [[CrossRef](#)]
124. Oh, S.E.; Logan, B.E. proton exchange and electrode surface areas as factors that affect power generation in microbial fuel cells. *Appl. Microbiol. Biotechnol.* **2006**, *70*, 162–169. [[CrossRef](#)]
125. Toczyłowska-Mamińska, R.; Pielech-Przybylska, K.; Sekrecka-Belniak, A.; Dziekońska-Kubczak, U. Stimulation of electricity production in microbial fuel cells via regulation of syntrophic consortium development. *Appl. Energy* **2020**, *271*, 115184. [[CrossRef](#)]

126. Krieg, T.; Enzmann, F.; Sell, D.; Schrader, J.; Holtmann, D. Simulation of the current generation of a microbial fuel cell in a laboratory wastewater treatment plant. *Appl. Energy* **2017**, *195*, 942–949. [[CrossRef](#)]
127. Stoll, Z.A.; Dolfig, J.; Xu, P. Minimum Performance Requirements for Microbial Fuel Cells to Achieve Energy-Neutral Wastewater Treatment. *Water* **2018**, *10*, 243. [[CrossRef](#)]
128. Sleutels, T.; Darus, L.; Hamelers, H.V.; Buisman, C.J. Effect of operational parameters on Coulombic efficiency in bioelectrochemical systems. *Bioresour. Technol.* **2011**, *102*, 11172–11176. [[CrossRef](#)] [[PubMed](#)]
129. Borole, A.P.; Hamilton, C.; Schell, D. Conversion of residual organics in corn stover-derived biorefinery streams to bioenergy via microbial fuel cells. *Environ. Sci. Technol.* **2013**, *47*, 642–648. [[CrossRef](#)] [[PubMed](#)]
130. Velasquez-Orta, S.B.; Yu, E.; Katuri, K.; Head, I.; Curtis, T.; Scott, K. Evaluation of hydrolysis and fermentation rates in microbial fuel cells. *Appl. Microbiol. Biotechnol.* **2011**, *90*, 789–798. [[CrossRef](#)]
131. Pannell, T.C.; Goud, R.K.; Schell, D.J.; Borole, A.P. Effect of fed-batch vs. continuous mode of operation on microbial fuel cell performance treating biorefinery wastewater. *Biochem. Eng. J.* **2016**, *116*, 85–94. [[CrossRef](#)]
132. Premier, G.C.; Kim, J.R.; Michie, I.; Dinsdale, R.M.; Guwy, A.J. Automatic control of load increases power and efficiency in a microbial fuel cell. *J. Power Sources* **2011**, *196*, 2013–2019. [[CrossRef](#)]
133. Marzorati, S.; Schievano, A.; Colombo, A.; Lucchini, G.; Cristiani, P. Ligno-cellulosic lingomaterials as air-water separators in low-tech microbial fuel cells for nutrients recovery. *J. Clean. Prod.* **2018**, *170*, 1167–1176. [[CrossRef](#)]
134. Velvizhi, G.; Mohan, S.V. Electrogenic activity and electron losses under increasing organic load of recalcitrant pharmaceutical wastewater. *Int. J. Hydrogen Energy* **2012**, *37*, 5969–5978. [[CrossRef](#)]
135. Watanabe, K. Recent Developments in Microbial Fuel Cell Technologies for Sustainable Bioenergy. *J. Biosci. Bioeng.* **2008**, *106*, 528–536. [[CrossRef](#)]
136. Wang, X.; Feng, Y.; Ren, N.; Wang, H.; Lee, H.; Li, N.; Zhao, Q. Accelerated start-up of two-chambered microbial fuel cells: Effect of anodic positive poised potential. *Electrochim. Acta* **2009**, *54*, 1109–1114. [[CrossRef](#)]
137. Elakkiya, E.; Matheswaran, M. Comparison of anodic metabolisms in bioelectricity production during treatment of dairy wastewater in Microbial Fuel Cell. *Bioresour. Technol.* **2013**, *136*, 407–412. [[CrossRef](#)]
138. Juang, D.F.; Yang, P.C.; Chou, H.Y.; Chiu, L.J. Effects of microbial species, organic loading and substrate degradation rate on the power generation capability of microbial fuel cells. *Biotechnol. Lett.* **2011**, *33*, 2147–2160. [[CrossRef](#)]
139. Yang, S.; Jia, B.; Liu, H. Effects of the Pt loading side and cathode-biofilm on the performance of a membrane-less and single-chamber microbial fuel cell. *Bioresour. Technol.* **2009**, *100*, 1197–1202. [[CrossRef](#)]
140. Sobieszuk, P.; Zamojska-Jaroszewicz, A.; Makowski, Ł. Influence of the operational parameters on bioelectricity generation in continuous microbial fuel cell, experimental and computational fluid dynamics modelling. *J. Power Sources* **2017**, *371*, 178–187. [[CrossRef](#)]
141. Ryu, J.; Lee, H.; Lee, Y.; Kim, T.; Kim, M.; Anh, D.; Tran, H.; Ahn, D. Simultaneous carbon and nitrogen removal from piggery wastewater using loop configuration microbial fuel cell. *Process. Biochem.* **2013**, *48*, 1080–1085. [[CrossRef](#)]
142. Hiegemann, H.; Lübken, M.; Schulte, P.; Schmelze, K.G.; Gredigk-Hoffmann, S.; Wichern, M. Inhibition of microbial fuel cell operation for municipal wastewater treatment by impact loads of free ammonia in bench-and 45 L-scale. *Sci. Total Environ.* **2018**, *624*, 34–39. [[CrossRef](#)]
143. Tice, R.C.; Kim, Y. Influence of substrate concentration and feed frequency on ammonia inhibition in microbial fuel cells. *J. Power Sources* **2014**, *271*, 360–365. [[CrossRef](#)]
144. Tao, Q.; Luo, J.; Zhou, J.; Zhou, S.; Liu, G.; Zhang, R. Effect of dissolved oxygen on nitrogen and phosphorus removal and electricity production in microbial fuel cell. *Bioresour. Technol.* **2014**, *164*, 402–407. [[CrossRef](#)] [[PubMed](#)]
145. Mashkour, M.; Rahimnejad, M. Effect of various carbon-based cathode electrodes on the performance of microbial fuel cell. *Biofuel Res. J.* **2015**, *2*, 296–300. [[CrossRef](#)]
146. Cheng, S.; Xing, D.; Logan, B.E. Electricity generation of single-chamber microbial fuel cells at low temperatures. *Biosens. Bioelectron.* **2011**, *26*, 1913–1917. [[CrossRef](#)]
147. Firdous, S.; Jin, W.; Shahid, N.; Bhatti, Z.A.; Iqbal, A.; Abbasi, U.; Ali, A. The performance of microbial fuel cells treating vegetable oil industrial wastewater. *Environ. Technol. Innov.* **2018**, *10*, 143–151. [[CrossRef](#)]
148. Bohn, I.; Björnsson, L.; Mattiasson, B. Effect of temperature decrease on the microbial population and process performance of a mesophilic anaerobic bioreactor. *Environ Technol.* **2007**, *28*, 943–952. [[CrossRef](#)]
149. Fang, Z.; Cao, X.; Li, X.; Wang, H.; Li, X. Biorefractory wastewater degradation in the cathode of constructed wetland-microbial fuel cell and the study of the electrode performance. *Int. Biodeterior. Biodegradation.* **2018**, *129*, 1–9. [[CrossRef](#)]
150. Shimoyama, T.; Komukai, S.; Yamazawa, A.; Ueno, Y.; Logan, B.E.; Watanabe, K. Electricity generation from model organic wastewater in a cassette-electrode microbial fuel cell. *Appl. Microbiol. Biotechnol.* **2008**, *80*, 325–330. [[CrossRef](#)] [[PubMed](#)]
151. Sciarria, T.P.; Vacca, G.; Tambone, F.; Trombino, L.; Adani, F. Nutrient recovery and energy production from digestate using microbial electrochemical technologies (METs). *J. Clean. Prod.* **2019**, *208*, 1022–1029. [[CrossRef](#)]
152. Wang, Y.; Lin, Z.; Su, X.; Zhao, P.; Zhou, J.; He, Q.; Ai, H. Cost-effective domestic wastewater treatment and bioenergy recovery in an immobilized microalgal-based photoautotrophic microbial fuel cell (PMFC). *Chem. Eng. J.* **2019**, *372*, 956–965. [[CrossRef](#)]
153. Jiang, H.; Luo, S.; Shi, X.; Dai, M.; Guo, R.B. A novel microbial fuel cell and photobioreactor system for continuous domestic wastewater treatment and bioelectricity generation. *Biotechnol. Lett.* **2012**, *34*, 1269–1274. [[CrossRef](#)]

154. Yakar, A.; Türe, C.; Türker, O.C.; Vymazal, J.; Saz, Ç. Impacts of various filtration media on wastewater treatment and bioelectric production in up-flow constructed wetland combined with microbial fuel cell (UCW-MFC). *Ecol. Eng.* **2018**, *117*, 120–132. [[CrossRef](#)]
155. Kim, J.R.; Zuo, Y.; Regan, J.M.; Logan, B.E. Analysis of ammonia loss mechanisms in microbial fuel cells treating animal wastewater. *Biotechnol. Bioeng.* **2008**, *99*, 1120–1127. [[CrossRef](#)] [[PubMed](#)]
156. Li, X.; Zhu, N.; Wang, Y.; Li, P.; Wu, P.; Wu, J. Animal carcass wastewater treatment and bioelectricity generation in up-flow tubular microbial fuel cells: Effects of HRT and non-precious metallic catalyst. *Bioresour. Technol.* **2013**, *128*, 454–460. [[CrossRef](#)]
157. Cord-Ruwisch, R.; Law, Y.; Cheng, K.Y. Ammonium as a sustainable proton shuttle in bioelectrochemical systems. *Bioresour. Technol.* **2011**, *102*, 9691–9696. [[CrossRef](#)]
158. Ichihashi, O.; Hirooka, K. Removal and recovery of phosphorus as struvite from swine wastewater using microbial fuel cell. *Bioresour. Technol.* **2012**, *114*, 303–307. [[CrossRef](#)]
159. Cusick, R.D.; Logan, B.E. Phosphate recovery as struvite within a single chamber microbial electrolysis cell. *Bioresour. Technol.* **2012**, *107*, 110–115. [[CrossRef](#)]
160. Hirooka, K.; Ichihashi, O. Phosphorus recovery from artificial wastewater by microbial fuel cell and its effect on power generation. *Bioresour. Technol.* **2013**, *137*, 368–375. [[CrossRef](#)] [[PubMed](#)]
161. Nelson, N.O.; Mikkelsen, R.L.; Hesterberg, D.L. Struvite precipitation in anaerobic swine lagoon liquids: Effect of pH and Mg: P ratio and determination of rate constant. *Bioresour. Technol.* **2003**, *89*, 229–236. [[CrossRef](#)]
162. Parsons, S.A.; Wall, F.; Doyle, J.; Oldring, K.; Churchley, J. Assessing the potential for struvite recovery at sewage treatment works. *Environ. Technol.* **2001**, *22*, 1279–1286. [[CrossRef](#)] [[PubMed](#)]
163. Güneş, K.; Weideler, A.; Krampe, J. Phosphorus recovery from digested sewage sludge as map by the help of metal ion separation. *Water Res.* **2008**, *42*, 4692–4698. [[CrossRef](#)]
164. Battistoni, P.; Pavan, P.; Prisciandaro, M.; Cecchi, F. Struvite crystallization: A feasible and reliable way to fix phosphorus in anaerobic supernatants. *Water Res.* **2000**, *34*, 3033–3041. [[CrossRef](#)]
165. Le Corre, K.S.; Valsami-Jones, E.; Hobbs, P.; Parsons, S.A. Phosphorus recovery from wastewater by struvite crystallization: A review. *Crit. Rev. Environ. Sci. Technol.* **2009**, *39*, 433–477. [[CrossRef](#)]
166. de-Bashan, L.E.; Bashan, Y. Recent advances in removing phosphorus from wastewater and its future use as fertilizer (1997–2003). *Water Res.* **2004**, *38*, 4222–4246. [[CrossRef](#)]
167. Yetilmezsoy, K.; İlhan, F.; Kocak, E.; Akbin, H.M. Feasibility of struvite recovery process for fertilizer industry: A study of financial and economic analysis. *J. Clean. Prod.* **2017**, *152*, 88–102. [[CrossRef](#)]
168. Doyle, J.D.; Parsons, S.A. Struvite formation, control and recovery. *Water Res.* **2002**, *36*, 3925–3940. [[CrossRef](#)]
169. Huchzermeier, M.P.; Tao, W. Overcoming challenges to struvite recovery from anaerobically digested dairy manure. *Water Environ. Res.* **2012**, *84*, 34–41. [[CrossRef](#)]
170. Sun, D.; Gao, Y.; Hou, D.; Zuo, K.; Chen, X.; Liang, P.; Zhang, X.; Ren, Z.; Huang, X. Energy-neutral sustainable nutrient recovery incorporated with the wastewater purification process in an enlarged microbial nutrient recovery cell. *J. Power Sources* **2018**, *384*, 160–164. [[CrossRef](#)]
171. Zhao, F.; Harnisch, F.; Schröder, U.; Scholz, F.; Bogdanoff, P.; Herrmann, I. Challenges and Constraints of Using Oxygen Cathodes in Microbial Fuel Cells. *Environ. Sci. Technol.* **2006**, *40*, 5193–5199. [[CrossRef](#)]
172. Hamza, R.A.; Zaghoul, M.S.; Iorhemen, O.T.; Sheng, Z.; Tay, J.H. Optimization of organics to nutrients (COD:N:P) ratio for aerobic granular sludge treating high-strength organic wastewater. *Sci. Total Environ.* **2019**, *650*, 3168–3179. [[CrossRef](#)]
173. Mei, X.; Xing, D.; Yang, Y.; Liu, Q.; Zhou, H.; Guo, C.; Ren, N. Adaptation of microbial community of the anode biofilm in microbial fuel cells to temperature. *Bioelectrochemistry* **2017**, *117*, 29–33. [[CrossRef](#)]
174. Babanova, S.; Jones, J.; Phadke, S.; Lu, M.; Angulo, C.; Garcia, J.; Carpenter, K.; Cortese, R.; Chen, S.; Phan, T. Continuous flow, large scale, microbial fuel cell system for the sustained treatment of swine waste. *Water Environ. Res.* **2020**, *92*, 60–72. [[CrossRef](#)]
175. Cusick, R.D.; Bryan, B.; Parker, D.S.; Merrill, M.D.; Mehanna, M.; Kiely, P.D.; Liu, G.; Logan, B.E. Performance of a pilot-scale continuous flow microbial electrolysis cell fed winery wastewater. *Appl. Microbiol. Biotechnol.* **2011**, *89*, 2053–2063. [[CrossRef](#)] [[PubMed](#)]
176. Liang, P.; Duan, R.; Jiang, Y.; Zhang, X.; Qiu, Y.; Huang, X. One-year operation of 1000-L modularized microbial fuel cell for municipal wastewater treatment. *Water Res.* **2018**, *141*, 1–8. [[CrossRef](#)]
177. Patel, D.; Bapodra, S.L.; Madamwar, D.; Desai, C. Electroactive bacterial community augmentation enhances the performance of a pilot scale constructed wetland microbial fuel cells for treatment of textile dye wastewater. *Bioresour. Technol.* **2021**, *332*, 125088. [[CrossRef](#)] [[PubMed](#)]
178. Zhuang, L.; Yuan, Y.; Wang, Y.; Zhou, S. Long-term evaluation of a 10-liter serpentine-type microbial fuel cell stack treating brewery wastewater. *Bioresour. Technol.* **2012**, *123*, 406–412. [[CrossRef](#)] [[PubMed](#)]
179. AlSayed, A.; Soliman, M.; Eldyasti, A. Microbial fuel cells for municipal wastewater treatment: From technology fundamentals to full-scale development. *Renew. Sustain. Energy Rev.* **2020**, *134*, 110367. [[CrossRef](#)]
180. Tan, W.; Chong, S.; Fang, H.-W.; Pan, K.-L.; Mohamad, M.; Lim, J.; Tiong, T.; Chan, Y.; Huang, C.-M.; Yang, T. Microbial Fuel Cell Technology—A Critical Review on Scale-Up Issues. *Processes* **2021**, *9*, 985. [[CrossRef](#)]
181. Kim, K.Y.; Rossi, R.; Regan, J.M.; Logan, B.E. Enumeration of exoelectrogens in microbial fuel cell effluents fed acetate or wastewater substrates. *Biochem. Eng. J.* **2021**, *165*, 107816. [[CrossRef](#)]

182. Lovley, D.R. Bug juice: Harvesting electricity with microorganisms. *Nat. Rev. Microbiol.* **2006**, *4*, 497–508. [[CrossRef](#)] [[PubMed](#)]
183. Fan, L.P.; Li, J.J. Overviews on internal resistance and its detection of microbial fuel cells. *Int. J. Circuits Syst. Signal Process.* **2016**, *10*, 316–320.
184. Niwa, M.; Pan, Z.; Shimamoto, S. IoT sensor network powered by sediment microbial fuel cell. In Proceedings of the IEEE 17th Annual Consumer Communications & Networking Conference (CCNC), Las Vegas, NV, USA, 10–13 January 2020; IEEE: Piscataway, NJ, USA, 2020; pp. 1–5.
185. Rahman, W.; Yusup, S.; Mohammad, S.N.A.A. Screening of fruit waste as substrate for microbial fuel cell (MFC). *AIP Conf. Proc.* **2021**, *2332*, 020003. [[CrossRef](#)]
186. Chen, W.; Liu, Z.; Li, Y.; Xing, X.; Liao, Q.; Zhu, X. Improved electricity generation, coulombic efficiency and microbial community structure of microbial fuel cells using sodium citrate as an effective additive. *J. Power Sources* **2021**, *482*, 228947. [[CrossRef](#)]
187. Koroglu, E.O.; Yoruklu, H.C.; Demir, A.; Ozkaya, B. Chapter 3.9-Scale-up and commercialization issues of the MFCs:challenges and implications. In *Microbial Electrochemical Technology*; Elsevier: Amsterdam, The Netherlands, 2019; pp. 565–583.
188. Rossi, R.; Logan, B.E. Unraveling the contributions of internal resistance components in two-chamber microbial fuel cells using the electrode potential slope analysis. *Electrochim. Acta* **2020**, *348*, 136291. [[CrossRef](#)]
189. Sleutels, T.; Ter Heijne, A.; Buisman, C.J.N.; Hamelers, H. Bioelectrochemical Systems: An Outlook for Practical Applications. *ChemSusChem* **2012**, *5*, 1012–1019. [[CrossRef](#)] [[PubMed](#)]
190. Torres, C.I.; Marcus, A.K.; Rittmann, B.E. Proton transport inside the biofilm limits electrical current generation by anode-respiring bacteria. *Biotechnol. Bioeng.* **2008**, *100*, 872–881. [[CrossRef](#)] [[PubMed](#)]
191. Ahmad, A.; Khatoon, A.; Umar, M.F.; Abbas, S.Z.; Rafatullah, M. Nanocomposite materials as electrode materials in microbial fuel cells for the removal of water pollutants. In *Emerging Carbon-Based Nanocomposites for Environmental Applications*; Mishra, A.K., Hussain, C.M., Mishra, S.B., Eds.; Wiley: Hoboken, NJ, USA, 2020; Chapter 9.
192. Qian, F.; Baum, M.; Gu, Q.; Morse, D.E. A 1.5 μ L microbial fuel cell for on-chip bioelectricity generation. *Lab Chip* **2009**, *9*, 3076–3081. [[CrossRef](#)]
193. Chang, M.H.; Chen, F.; Fang, N.S. Analysis of membraneless fuel cell using laminar flow in a Y-shaped microchannel. *J. Power Sources* **2006**, *159*, 810–816. [[CrossRef](#)]
194. Chen, F.; Chang, M.H.; Lin, M.K. Analysis of membraneless formic acid microfuel cell using a planar microchannel. *Electrochim. Acta* **2007**, *52*, 2506–2514. [[CrossRef](#)]
195. Nath, D.; Kallepalli, S.; Rao, L.T.; Dubey, S.K.; Javed, A.; Goel, S. Microfluidic paper microbial fuel cell powered by *Shewanella putrefaciens* in IoT cloud framework. *Int. J. Hydrogen Energy* **2021**, *46*, 3230–3239. [[CrossRef](#)]
196. Nguyen, T.; Arias-Thode, Y.M.; Obraztsova, A.; Sarmiento, A.; Stevens-Bracy, A.; Grbovic, D.; Kartalov, E.P. Proof-of-concept for a novel application for in situ microfluidic benthic microbial fuel cell device (MBMFC). *J. Environ. Chem. Eng.* **2021**, *9*, 105659. [[CrossRef](#)]
197. Aelterman, P.; Rabaey, K.; Pham, H.T.; Boon, N.; Verstraete, W. Continuous electricity generation at high voltages and currents using stacked microbial fuel cells. *Environ. Sci. Technol.* **2006**, *40*, 3388–3394. [[CrossRef](#)] [[PubMed](#)]
198. Jadhav, D.A.; Das, I.; Ghangrekar, M.M.; Pant, D. Moving towards practical applications of microbial fuel cells for sanitation and resource recovery. *J. Water Process Eng.* **2020**, *38*, 101566. [[CrossRef](#)]